5. Appendix A: Completed DD Form 298

REPORT DOCUMENTATION PAGE

Form Approved
OMB NO. 0704-0188

1. AGENCY USE ONLY (Leave Blank)	2. REPORT DATE	3. REPORT TYPE AND DATES COVERED
	July 31, 2007	Final Progress Report, Oct 1 2006 – June 30 2007

4. TITLE AND SUBTITLE
Experimental Verification of a Systematic Method for Identifying Contact-Dynamics Model Parameters

5. FUNDING NUMBERS
W911NF-06-1-0492

6. AUTHOR(S)
Ou Ma

7. PERFORMING ORGANIZATION NAME(S) AND ADDRESS(ES)
New Mexico State University, College of Engineering
P.O. Box 30001, Las Cruces, NM 88003

8. PERFORMING ORGANIZATION REPORT NUMBER

9. SPONSORING / MONITORING AGENCY NAME(S) AND ADDRESS(ES)
U. S. Army Research Office
P.O. Box 12211
Research Triangle Park, NC 27709-2211

10. SPONSORING / MONITORING AGENCY REPORT NUMBER
50388.2-EG-II

11. SUPPLEMENTARY NOTES
The views, opinions and/or findings contained in this report are those of the author(s) and should not be construed as an official Department of the Army position, policy or decision, unless so designated by other documentation.

12 a. DISTRIBUTION / AVAILABILITY STATEMENT
Approved for public release; distribution unlimited.

12 b. DISTRIBUTION CODE

13. ABSTRACT (Maximum 200 words)

This project is aimed at conducting an experimental test of a new and systematic method for identifying the key parameters of a general multiple-point contact dynamics model using a robotics-based experimental testbed. The hypothesis verified in this project is that the identification method is capable of identifying the stiffness, damping, and friction parameters all together from a same hardware test. Such an identification capability is very appealing to physical simulation practice because the existing technologies allow identify these parameters from hardware test only one at a time using special equipment. Therefore, the new method can significantly increase the efficiency and convenience of simulation practice. The theoretical part of the method was developed earlier and it had also been tested using computer simulations. In this short-term project, the method was experimentally investigated using a specially designed hardware setup. Because of the time limitations of the STIR program, the test could only be done with one- and two-point contact cases. Nevertheless, these tests have experimentally demonstrated the feasibility of the method.

14. SUBJECT TERMS	15. NUMBER OF PAGES
Contact dynamics, parameter identification, experiment, verification, simulation	9 – the main report 41 – including appendices
	16. PRICE CODE

17. SECURITY CLASSIFICATION OR REPORT	18. SECURITY CLASSIFICATION ON THIS PAGE	19. SECURITY CLASSIFICATION OF ABSTRACT	20. LIMITATION OF ABSTRACT
UNCLASSIFIED	**UNCLASSIFIED**	**UNCLASSIFIED**	**UL**

NSN 7540-01-280-5500

Standard Form 298 (Rev.2-89)
Prescribed by ANSI Std. 239-18
298-102

FINAL PROGRESS REPORT

for

ARO Research Contract **#W911NF-06-1-0492 (Project #50388-EG-II)**

Project Title: Experimental Verification of a Systematic Method for Identifying Contact-Dynamics Model Parameters

Ou Ma

Department of Mechanical Engineering, New Mexico State University
P.O. Box 30001, MSC 3450, Las Cruces, NM 88003
Tel.: (505)646-6534, Email: oma@nmsu.edu

Table of Contents

1. Statement of the Problem Studied

This project is aimed at conducting an experimental verification of a new and systematic method for identifying contact dynamics model parameters using a robotics-based experimental testbed.

The hypothesis verified by the project is that the identification method is capable of identifying the stiffness, damping, and friction parameters all together from the same hardware test.

Simultaneously identify multiple contact parameters directly from a physical test of a dynamical system is desirable in practice because the existing technology allows to identify the same parameters only one at a time using special equipment and skilled labors, which is very inconvenient and costly. Therefore, the new method, if experimentally proven working, can significantly increase the efficiency and convenience of modeling and simulation tasks. The theoretical part of the identification method was developed earlier but had not been experimentally verified prior to this project. In this short-term project, the method is experimentally tested using a specially designed experiment setup. Because of the funding and time limitations of the ARO's STIR program, the test could only be limited to a basic level with one- and two-point contact cases. Nevertheless, these tests can still demonstrate the feasibility of the method.

2. Summary of the Results

2.1 Approach

The basic approach of the identification method is to use the linear estimation technology to identify the stiffness, friction, and damping parameters from the relative pose (both position and orientation) and velocity as well as the resultant contact force and moment between two arbitrary contacting bodies. The key is that the method estimates the locations of all individual contact points by combining the measured motion data and the known geometry data of the two contact bodies. In such a manner the very difficult problem of measuring all simultaneous and unperceived contact locations and forces is converted to a much less difficult problem of measuring the rigid-body motion and resultant contact force-moment of a contact body. This is a breakthrough in dealing with the general multi-point contact problem in the identification procedure. (Detailed information about the approach is presented in Section 2.2 of the attached technical report in Appendix B.)

In this project, we tested the method using a specially designed, robotics-based experimental testbed as shown in Figs. 1 and 2. The robotic arm is used to generate controlled and repeatable contact motion in 3-D space, so that general contact scenarios can be tested. The 3-D motion tracking system is used to measure the 3D pose and velocity of the moving contact body and a 6-axis force-moment sensor is used to measure the resultant contact force and moment. This testbed was designed and built based on the special requirements for the verification of the identification method. (More detailed information about the testbed is presented in Section 3 of the attached technical report in Appendix B.)

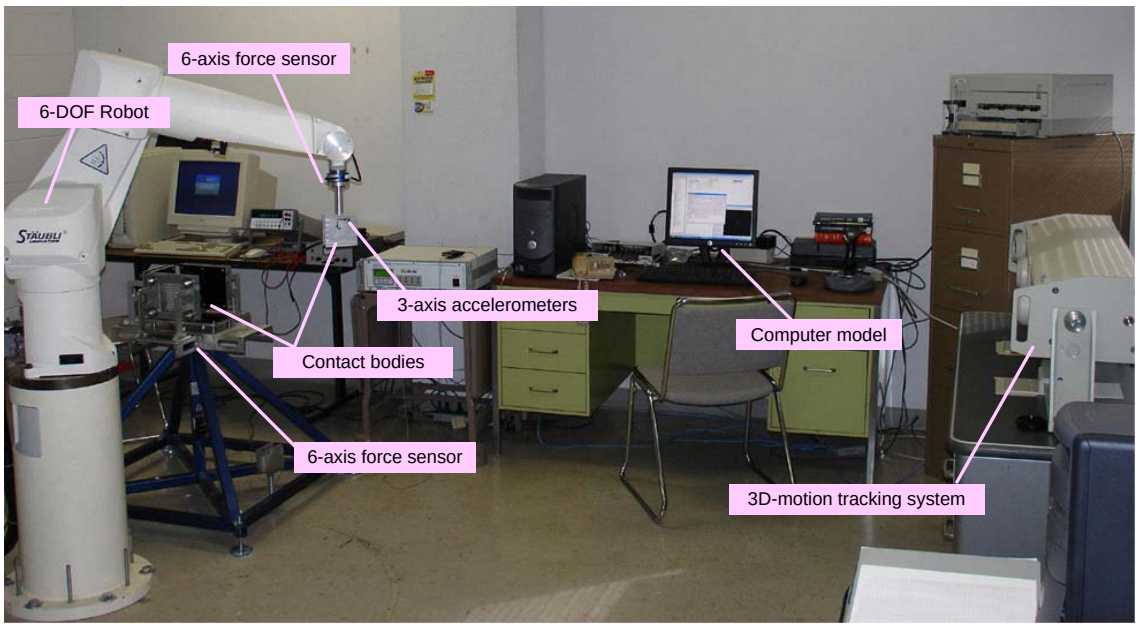

Figure 1. Integrated hardware system of the contact-parameter identification experiment testbed

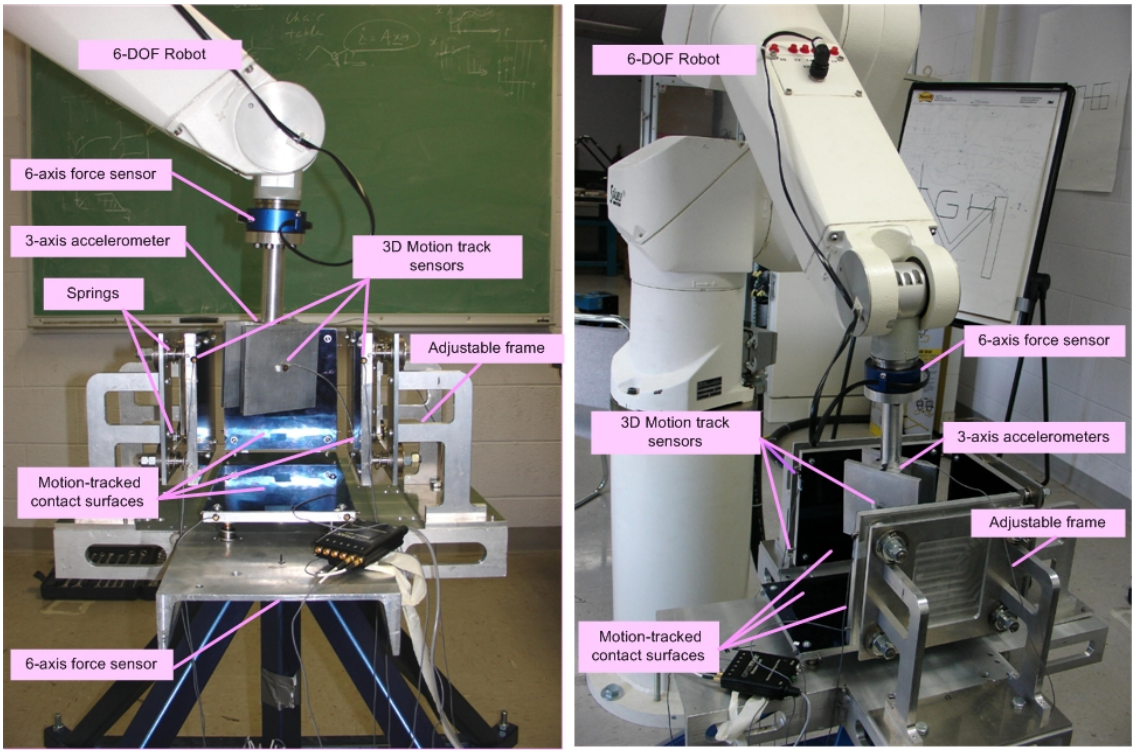

Figure 2. The instrumented contact interfaces of the testbed

2.2 Accomplishments

The accomplishments of the project are briefly summarized as follows:

(1) Completed the hardware-software integration of the test system so that the entire experimental system is up and running.

(2) Tested the single-point contact case.

Various tests indicated that the stiffness, damping and friction parameters can be simultaneously identified within a relative error of 2%, 6% and 4%, respectively. In modeling and simulation practice for contact dynamics systems, such an accuracy level is usually acceptable.

(3) Tested the two-point contact case.

Various tests indicated that the two sets of stiffness, damping and friction parameters can be simultaneously identified within error ranges of 2~3%, 15~25% and 5~7%, respectively. Again, such an accuracy level for the stiffness and friction parameters is usually acceptable but that for the damping parameters is too low.

(4) Investigated the error sources.

It was found that the above-mentioned errors were mainly caused by imperfect design and fabrication of the test hardware. Part of the errors was caused by without considering the static friction in the approach[1]. The latter cause is related to the identification method and thus, should be corrected in the future research.

(Detailed test results and discussions about identification errors can be found in Sections 4 and 5 of the attached technical report in Appendix B.)

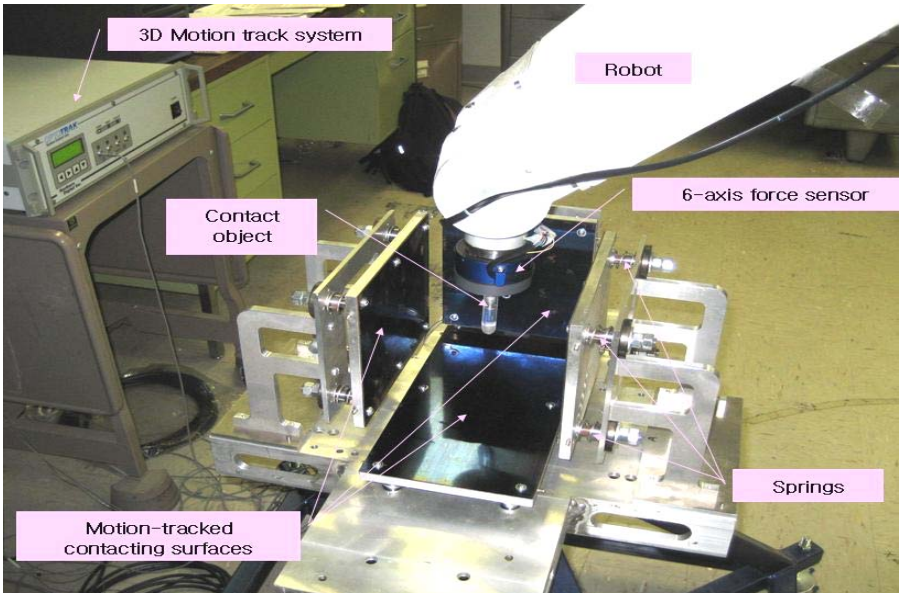

Figure 3 Instrumented contact interface for testing multiple-point contact dynamics

[1] Identification of static friction parameters was not planned in the first place. Since static friction is very nonlinear, the linear-estimation based identification approach has to be significantly modified in order to deal the problem. Hence, further research is needed.

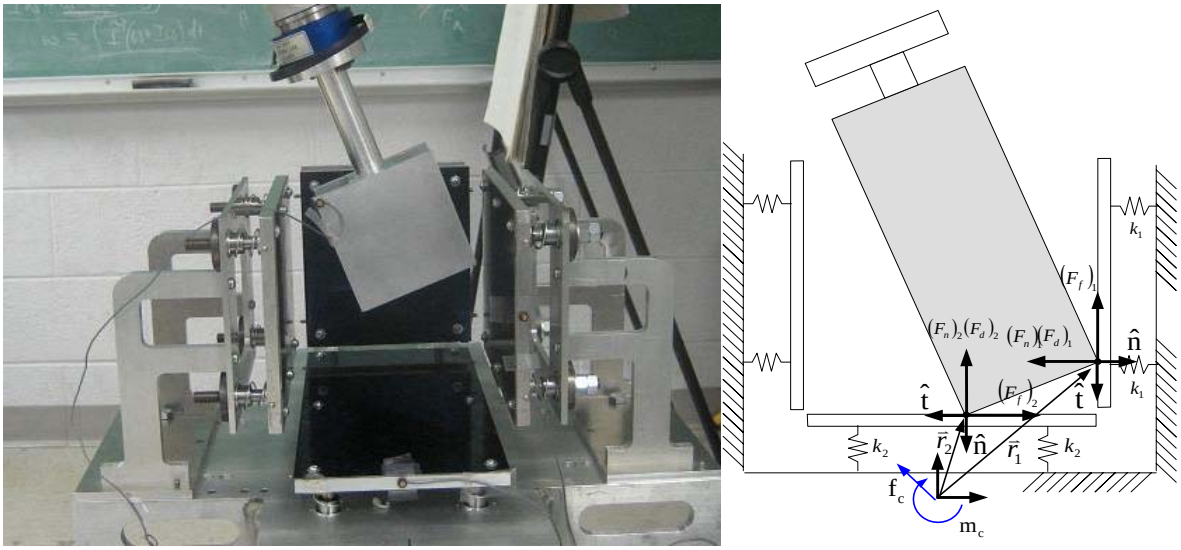

Figure 4 Instrumented contact interface for testing multiple-point contact dynamics

2.3 Significance

The significance of this research can be summarized as follows:

(a) **Uniqueness:** The method of simultaneously identifying all the three major contact parameters (i.e., the stiffness, damping and friction parameters) from a single hardware test is unique. The experimental verification of such a method is also unique. To our best knowledge, it has never been done elsewhere.

(b) **Efficiency:** using the proposed parameter identification method, multiple stiffness, damping, and friction parameters of a complicated contact case can be identified all together. On the contrary, all the other available methods have to identify these parameters one by one separately using special measurement equipment. Therefore, the new method is obviously more efficient and convenient.

(c) **Effectiveness:** This research project has demonstrated that the new identification method works robustly (at least in the lab environment) although some further research may be needed in order to improve the accuracy level.

(d) **Army Applications:** With the fast advancement of general computation and simulation technology, physical simulation will be playing more and more roles in the design, verification and even operation of future military systems. More accurate model parameters are always required for better simulation-based prediction. The studied parameter identification method is a more convenient, efficient, and cost-saving tool than any other existing parameter identification tools to enhance physical simulations.

2.4 Innovation

The proposed research addresses a challenging parameter identification problem which is encountered by industry nowadays because simulation models are increasingly becoming more complex and essential in a product development cycle while the traditional methods of

measuring individual parameters separately become very inefficient. The tested method solves this problem by allowing simultaneous identification of multiple contact-dynamics parameters directly from routine hardware test and thus, it improves efficiency and quality of modeling and simulation. This will have a broader impact on industry (especially the defense and aerospace industries) where simulation plays critical roles in design, verification, and even operation phases. The key innovative parts of the approach are:

(1) avoided sensing all simultaneous but unperceived local contact points and forces by just sensing the overall rigid-body motion and resultant contact force information;

(2) incorporated known geometric model into identification process so that the contact bodies can be as complicated as a geometric model can describe;

(3) used a robotics-based testbed to perform the most general 3-D verification testing.

In short, the identification method is new, the experimental study has not been done elsewhere, and the research output is relevant to the Army. Therefore, this research effort is in line with ARO's basic research goal – develop new and better technology to support national defense.

2.5 Enhancement to Education

Two graduate students were trained in the project. One of them, Jong Kim, just completed his M.Sc. degree in May 2007. This research project is exactly the topic of his master's thesis. Another master's student, Lucas Martinez, also worked on the project. He will be graduating in fall 2007. Although this short project finished, the research will go on and thus more students will be trained in the lab in the future.

Moreover, the experiment system developed and used in this project can always be used as a teaching tool for class demonstrations and course projects.

2.6 Enhancement to Other Research

The hardware testbed has become part of the experimental infrastructure supporting research in multibody dynamics, robotics and controls in the Robotics Lab of NMSU. Dr. Ma and his research group are currently using the lab facility for research in:

(1) contact-impact dynamics model parameters identification

(2) hardware-in-the-loop contact dynamics simulation

(3) automatic identification of inertia properties

(4) development of compliance control technology

2.7 Technology Transfer

It is difficult for such a short-term basic research to have led to a materialized technology transfer. However, Dr. Ma has been making efforts to inform the ARL and industry about this research and other related research for potential technology transfer and further research collaboration. For example,

- Dr. Ma continues to communicate with Dr. David Lamb of ARL/TACOM about the research on contact dynamics modeling and simulation for dynamical systems. From Dr. Lamb, he learned that ARL/TACOM is still interested in developing contact-dynamics simulation capabilities but with more focus on real-time simulation. Dr. Ma responded this updated need by proposing a research on the topic of model order reduction for contact dynamics simulations. Such a research is aimed at significantly improving the simulation speed, so that real-time simulation can become possible. Dr. Ma is planning to visit ARL/TACOM in the near future.
- Dr. Ma visited the ARL/APG (invited by Dr. Raju Namburu) in Aberdeen, MD, on May 15, 2007, and gave a presentation about his contact dynamics research including some highlights of this project. From the visit, Dr. Ma gets connected with some of the researchers in APG, which will help develop potential future research collaboration.
- Dr. Ma participated the 17'th Army Symposium on Solid Mechanics in Baltimore, MD, April 2-5, 2007 and presented some of the research results of this project. Through the symposium, he learned various ARO funded research activities and see a bigger picture of the current Army research needs. This will help him to orient his research to better in line with the Army's research priorities.
- Dr. Ma also talked with some peers in defense industry. For example, he discussed the identification technology with Dr. Pejmun Motaghedi of Boeing in Huntington Beach, CA. Due to his industrial experience, Dr. Motaghedi fully understood and appreciated this research. He wrote an official support letter for Dr. Ma. Another industrial expert, Dr. James Turner of Dynacs Inc. in Houston, TX, also realized the importance of this research and also wrote a support letter.

3. Participating Scientific Personnel

Dr. Ou Ma, the PI of the project, is the co-developer of the identification method tested by the project and the designer of the experimental verification system. He managed the project and provided scientific guidance for the other participants on daily basis. Dr. Ma is specialized in multibody dynamics and controls for the applications of robotic systems. He has over ten years' industrial experience and five years' academic experience in developing and verifying contact dynamics modeling and simulation technology for complicated dynamical systems. He has over sixty peer-reviewed publications and over 200 ISI journal citations.

Mr. Jong Kim is a graduate student who just received his M.Sc. degree in May 2007 from NMSU. He has been the main participant of the project responsible for the most part of the experimental work.

Mr. Lucas Martinez is a graduate student who is pursuing M.Sc degree at NMSU. He helped with some of the hardware integration. Lucas will continue to work in the lab until graduation scheduled in the end of 2007. He will then join the Air Force Research Lab in Florida.

4. List of Publications

To disseminate the new technology, the findings of this research have been documented in a M.Sc. thesis and several technical papers to be published, as listed below:

[1] Jong Hwan Kim, “Experimental Investigation of a Systematic Method for Identifying Multiple Contact Model Parameters”, M.Sc. Thesis, Department of Mechanical Engineering, New Mexico State University, May 2007.

[2] O. Ma, “Test of a Systematic Method of Identifying Multiple Contact-Dynamics Parameters”, a presentation at the 17’th US Army Symposium on Solid Mechanics, Baltimore, MD, April 2-5, 2007.

[3] O. Ma and J. Kim “A robotics-based testbed for verifying a systematic method of identifying contact-dynamics model parameters”, to be published in the ASME International Design Engineering Technical Conferences and Computers and Information Conference (IDETC), Sept.4-7, 2007, Las Vegas, NV, Paper #DETC2007-35092.

[4] J. Kim, O. Ma and L. Martinez, “Experimental verification of a method for identifying contact-dynamics model parameters from multiple-point contact testing”, a journal paper currently in preparation.

The funding support from the Army Research Office has been acknowledged in all of the above listed documents and publications.

Final Technical Report for Research Grant #50388-EG-II

Experimental Verification of a Systematic Method for Identifying Contact-Dynamics Model Parameters

Ou Ma
Ph.D. and Associate Professor, Department of Mechanical Engineering
New Mexico State University, Las Cruces, New Mexico 88005

Jong Kim and Lucas Martinez
Graduate Students, Department of Mechanical Engineering
New Mexico State University, Las Cruces, New Mexico 88005

July 30, 2007

EXECUTIVE SUMMARY

This technical report describes the results of a 9-month research project conducted by Dr. Ou Ma and his graduate students at the New Mexico State University under the ARO grant Research Grant #50388-EG-II starting on September 30, 2006 and ending on June 30, 2007.

This project is aimed at conducting an experimental test of a new and systematic method for identifying the key parameters of a general multiple-point contact dynamics model using a robot-based experimental testbed. The hypothesis to be verified is that the identification method is capable of identifying the stiffness, damping, and friction parameters all together from a same hardware test. Such a capability is appealing in practice because the existing technology allows to identify these parameters from experiment only one at a time using special equipment. Therefore, the new technology, if experimentally proven working, can significantly increase the efficiency and convenience of modeling and simulation tasks. The theoretical part of the method was developed earlier and it had also been tested using computer simulations. In this short-term project, the method was experimentally tested using a specially designed hardware setup. Because of the funding and time limitations of the STIR program, the test could only be limited to basic level with one- and two-point contact cases. Nevertheless, such tests are sufficient to demonstrate the feasibility of the method.

This technical report describes:

1) the theory and procedure of the parameters identification method;
2) the basic requirements of the intended experiment and how they are met by the design of the experiment testbed.
3) the results of the experimental testing of the identification method obtained so far.
4) a conclusion drawn from the test results and discussion about further research in this direction

In conclusion, the test results demonstrated that the method can identify all the three unknown contact parameters simultaneously with small errors. Investigation indicates that the errors are mainly caused by the imperfect design and hardware implementation of the test system as opposed to the identification method itself.

TABLE OF CONTENTS

1. INTRODUCTION

Physical contact (including nondestructive impact) with environment or external objects for a military vehicle is not only very possible but sometimes also a part of an operation in an urban battlefield. Here, among many, are several examples of contact scenarios,

A land vehicle pinned and struggling between obstacles, a ditch, or other vehicles.

A land vehicle hitting obstacles such as barriers, building debris, walls, trees, etc.

A land or aerial vehicle being hit by flying or falling objects.

An aerial vehicle landing or accidentally colliding with a tree, a tower, a building, etc.

Contact may cause severe damage to crew, onboard equipment, or the structure of a dynamic system. In addition, contact phenomena are also among the most difficult operational scenarios for the operators and control systems to handle. In order to predict the consequence and minimize the negative impact of physical contact, engineers need to thoroughly study various contact scenarios and their effects on the associated dynamic systems. Obviously, computer simulation is the safest and effective means for investigating such scenarios. Contact dynamics simulation has been playing and will be increasingly playing an essential role in the development and operation of robotic and vehicular systems operating in extreme environments such as space, under sea, and battle field. Based on a decade-long hands-on experience in conducting high-fidelity contact dynamics modeling and simulations for robotic systems in industry, we have seen many limitations on the current technologies affecting the efficiency, fidelity, and performance of contact dynamics simulations of complex systems. One of such limitations is lack of a systematic and practical methodology for identifying different model parameters all together efficiently from the system-level test of a physical prototype or the final physical system. This project is part of the effort that our research group is currently making to addresses this problem.

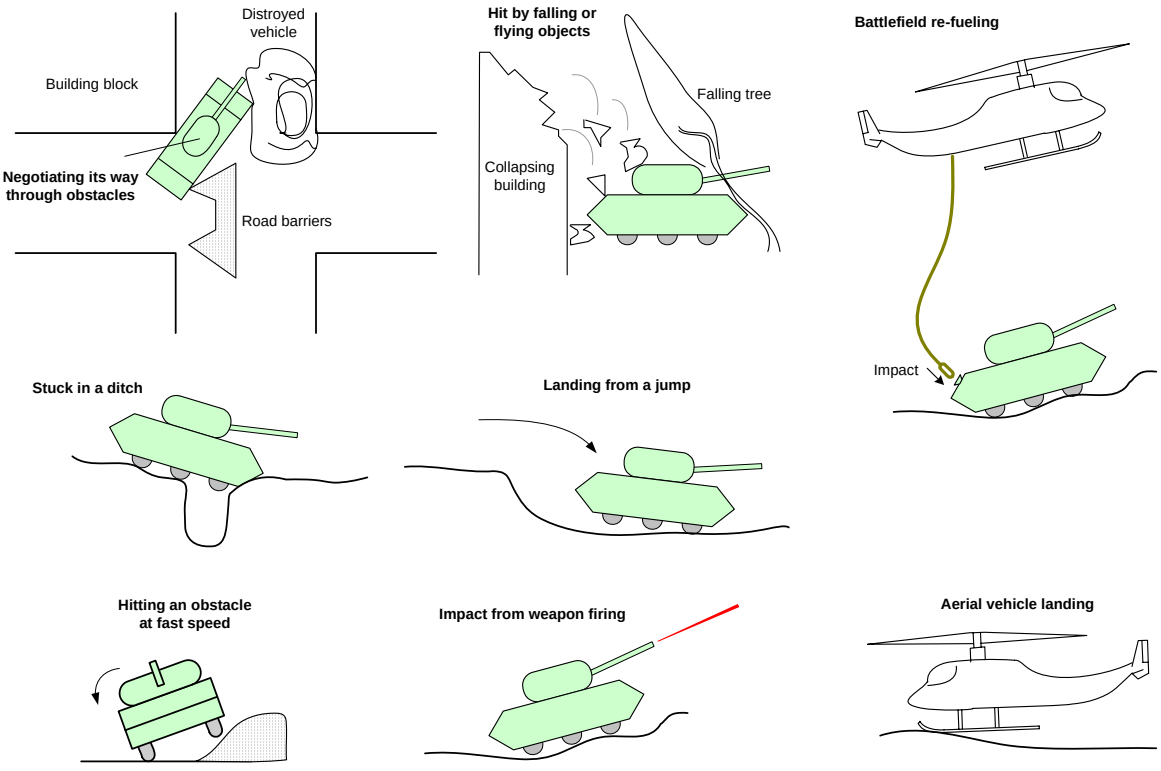

Figure 1. Examples of possible contact scenarios in army operations

The accuracy of a dynamic simulation depends not only on the mathematical model (i.e., formulation, algorithms, and computer code) but also on the values of model parameters. A contact-dynamics model of a dynamical system for military applications, such as the ones shown in Fig.1, can have many different model parameters. Determination of these parameters for such a large and complex system is a large challenge. Similar examples exist across the aerospace, defense, and automobile industries, where high fidelity contact-dynamics simulations are essential in support of the design, verification, and even operations but there are no systematic and easy-to-use techniques available to identify model parameters directly from system level hardware tests. Researchers have usually focused their efforts of contact-dynamics research on developing solution methods/algorithms and verifying their algorithms by experiments. Much less focus has been placed on developing systematic methods of measuring model parameters for multiple-point contact scenarios. Similarly, most of the commercial software packages for dynamic simulations nowadays, such as ADAMS, DADS, SIMPACK, Working Model, etc., are offering contact-dynamics modeling and simulation capabilities. However, to the best knowledge of the authors, none of them provides supplementary software tools to assist the users identifying or tuning their model parameters using experiment data. In reality, some of the contact-dynamics model parameters used in industry are not directly measured from the real hardware in representative operation conditions due to lack of adequate measurement techniques. Instead, those parameters were assumed based on the design data or engineers' best guess. Such a practice will add uncertainties to the fidelity of the corresponding simulation model. As a result, a system designed or a mission planned based on such a simulation practice would have to bare extra safety margins and thus is not optimized. Therefore, there exists a strong desire in industry for a practical means of systematically identifying multiple model parameters. The PI of this research project, while he was employed in industry a few years ago, initiated a university-industry collaborative research project on this topic. As a result, a method of identifying multiple contact-dynamics parameters was developed and demonstrated by simulation study (Weber, Patel, Ma and Sharf 2006). This project is aimed at experimental investigation of this method. Because of the small scope of this STIR project, the investigation can only be limited to a preliminary level.

The basic approach of the identification method experimentally investigated on this project has been described in (Weber, Patel, Ma, and Sharf 2006). It uses the linear estimation technology to identify the stiffness, friction, and damping parameters from the relative pose (both position and orientation) and velocity as well as the resultant contact force between two arbitrary contacting bodies. The key is that the method estimates the locations of all individual contact points by combining the measured motion data and the known geometry data of the two contact bodies. In such a manner the very difficult problem of measuring all simultaneous and unperceived contact locations and forces is converted to a much less difficult problem of measuring the rigid-body motion and resultant wrench (both force and moment) of each of the two contact bodies. This is a breakthrough in dealing with the general multi-point contact problem in the identification procedure. A simulation study of the method has shown promising results. In this project, we tested the method using a specially designed, robotics-based experimental testbed.

2. THEORY

2.1 Contact Dynamics Modeling

To help describe the identification method, it is necessary to have a brief overview of the related modeling approach of contact dynamics. In the approach, each contact region or area is assumed to be much smaller than the size of the involved contact body and thus the contact region can be approximated by a point called "contact point". The contact is then modeled by a spring-damper model with a friction component. The contact force at the contact point is the resultant of three individual forces, namely,

$$\mathbf{f}_c = \mathbf{f}_n + \mathbf{f}_d + \mathbf{f}_f \tag{1}$$

where $\mathbf{f}_n$, $\mathbf{f}_d$, and $\mathbf{f}_f$ are the 3D vectors of normal, damping, and friction forces, respectively, all acting at the same point, as shown in Fig.2. Details of the individual forces can be found from many references such as (Brach 1991; Freeman and Orin 1991; Kraus and Kumar 1996; Ma et al 1997; Song et al 2001; and Gonthier, McPhee, and Lange 2004). A highlight of the model is given below for quick reference. The most commonly seen model of the normal force is the Hertz model

$$\mathbf{f}_n = -k_c d^{\lambda} \mathbf{n} \tag{2}$$

where k_c and d are the contact stiffness and contact-surface deformation (i.e., deflection of the "spring"); exponent λ depends on contact geometry (Gilardi and Sharf 2002); and n is an out-pointing effective normal vector weighted from the normal vectors of all the surfaces (faces) involved in the associated contacting region.

The contact damping force accounts for energy loss during the contact. It is assumed to be proportional to the rate of the surface deformation and always against the direction of the deformation rate, namely,

$$\mathbf{f}_d = -c\dot{d}\mathbf{n} \tag{3}$$

where c is the contact damping coefficient and $\dot{d}$ is the time rate of the surface deformation (also called indentation) d. A nonlinear damping model may be introduced to prevent the contact force $\mathbf{f}_c$ from becoming an attractive force when the impact speed is high (Marhefka and Orin 1999).

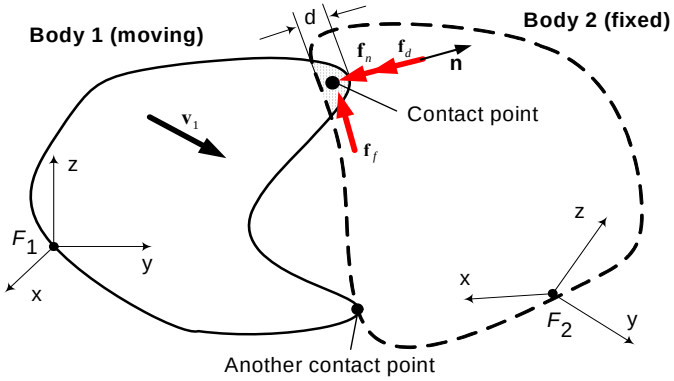

Figure 2. Local contact force components

The kinetic friction force is modeled using the following friction force model

$$\mathbf{f}_f = -\mu f_n \frac{\mathbf{v}_t}{|\mathbf{v}_t|}, \quad (\mathbf{v}_t \neq \mathbf{0}) \tag{4}$$

where μ is the kinetic friction coefficient; f_n is the magnitude of the normal force; and $\mathbf{v}_t$ is the tangential velocity between the two contact bodies at the contacting point. Basically, this is the Coulomb friction model which works for sliding friction only. During a contact between two objects, the two contact bodies may not have relative velocity at their contacting point, such as in a jamming or stick-slip situation. In such a case, the static friction is in play. A more general friction model called 3D integrated bristle friction model was introduced in (Ma et al. 1997) to represent both the sliding friction and static friction. However, the model has not yet been considered in the parameters identification so far because of its complexity.

The amount of the surface deformation of the contacting point is approximated by computing the 3D geometric intersection (also called geometric interference or indentation) of the two contact bodies assuming they are rigid bodies in the geometry computation. Two methods are available to compute the variables of such a geometric intersection including the dimensions, surface areas, and volume. The first method is called shrinking-body method which was introduced by Liu and Mayne (1990) and extended by

Nahon (1994). The method shrinks the two contact bodies along their surface normal directions until the two intersecting bodies become just touch at a single point. The amount of the shrinking of each body is considered as the deflection of that body and the resulting touching point is considered as the contact point where all the contact forces defined in (1) are applied to. The second method uses the duality technique and convex hull theory (Preparata and Shamos 1985; O'Rourke 1993) to calculate the geometric intersection between the two bodies but it is applicable to bodies with linear bounding surfaces only. The method has been widely used in computer graphics and CAD software tools. Recently, Luo and Nahon (2005) used the method to approximate the surface deformation for contact-dynamics modeling. In principle, both methods apply to convex bodies only. This is not a problem because, in practice, a non-convex body can always be divided into or approximated by several convex sub-bodies (Ma et al, 1997).

2.2 Parameters Identification Method

The general method of contact-dynamics modeling outlined in Section 2.1 requires three principal parameters for each pair of contact bodies or subbodies. They are contact stiffness, contact damping coefficient, and sliding friction coefficient. In this section an algorithm for simultaneously identifying these parameters from experiment data collected from hardware testing is presented. A contact must involve at least two bodies and both of them may move during the contact activity. Without loss of generality and for the convenience of conceptual description here, it is assumed that one of the two contacting bodies is fixed and the other body moves with respect to the fixed body. Note that in the real implementation and experiment, the absolute motions of both bodies can be measured by 3D motion sensors, from which the relative motion between the two bodies can be easily obtained.

2.2.1 Relation between Contact Wrench and Model Parameters

It is assumed that there are n simultaneous contact points, as shown in Fig.3, and n varies over the time depending on the relative motion between the two contact bodies. The resultant contact force and moment with respect to a specific reference point and frame can be expressed in terms of the individual local contact forces in the following form,

$$\begin{aligned} \mathbf{f}_c &= \sum_{i=1}^{n} \mathbf{f}_{ci} = \sum_{i=1}^{n} \left[\mathbf{f}_{ni} + \mathbf{f}_{di} + \mathbf{f}_{fi} \right] \\ \mathbf{m}_c &= \sum_{i=1}^{n} \mathbf{r}_i \times \mathbf{f}_{ci} = \sum_{i=1}^{n} \mathbf{r}_i \times \left(\mathbf{f}_{ni} + \mathbf{f}_{di} + \mathbf{f}_{fi} \right) \end{aligned} \tag{5}$$

where $\mathbf{f}_c$ and $\mathbf{m}_c$ are the resultant contact force and moment resolved at a specific reference point (usually defined for the convenience of the modeling procedure); $\mathbf{f}_{ni}$, $\mathbf{f}_{di}$, and $\mathbf{f}_{fi}$ are the local contact normal force, damping force, and friction force applied at the *i*th contact point; and *n* is the total number of simultaneous contact points. The application locations or points of these local contact forces depend on the geometries and motion states of the two involved contact bodies.

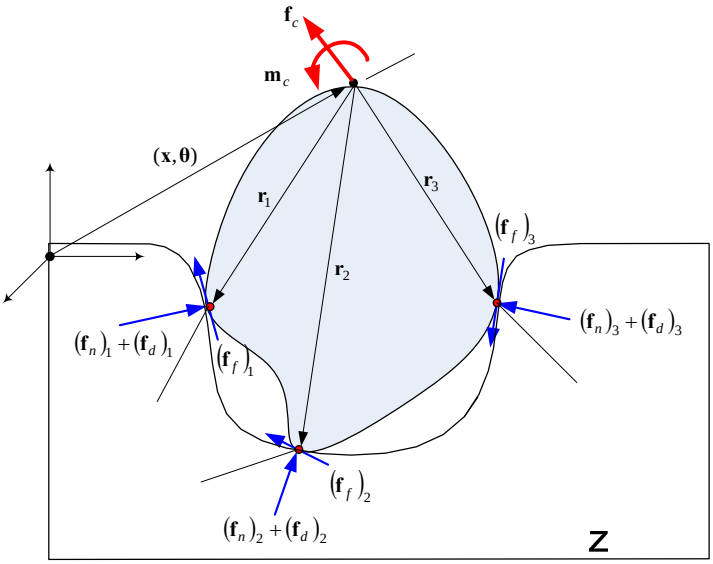

Figure 3. Individual local contact forces and their resultant force-moment resolved at a reference point

With the application of the force models defined in Section 2, equation (5) can be rewritten into the following form

$$\begin{aligned}
\mathbf{f}_c &= \sum_{i=1}^{n}\left[k_i d_i^{\lambda}\mathbf{n}_i + c_i\dot{d}_i\mathbf{n}_i + \mu_i k_i d_i^{\lambda}\mathbf{t}_i\right] \\
&= \sum_{i=1}^{n}\left[\left(d_i^{\lambda}\mathbf{n}_i\right)k_i + \left(\dot{d}_i\mathbf{n}_i\right)c_i + \left(d_i^{\lambda}\mathbf{t}_i\right)k_i\mu_i\right] \\
\mathbf{m}_c &= \sum_{i=1}^{n}\mathbf{r}_i\times\left[k_i d_i^{\lambda}\mathbf{n}_i + c_i\dot{d}_i\mathbf{n}_i + \mu_i k_i d_i^{\lambda}\mathbf{t}_i\right] \\
&= \sum_{i=1}^{n}\left[\left(d_i^{\lambda}\mathbf{r}_i\times\mathbf{n}_i\right)k_i + \left(\dot{d}_i\mathbf{r}_i\times\mathbf{n}_i\right)c_i + \left(d_i^{\lambda}\mathbf{r}_i\times\mathbf{t}_i\right)k_i\mu_i\right]
\end{aligned} \tag{6}$$

For the convenience of computing the unknown model parameters, the above equations can be rewritten into the following linear equations in terms of model parameters

$$\begin{aligned}
\begin{bmatrix}\mathbf{f}_c\\ \mathbf{m}_c\end{bmatrix} &= \sum_{i=1}^{n}\begin{bmatrix} d_i^{\lambda}\mathbf{n}_i & \dot{d}_i\mathbf{n}_i & d_i^{\lambda}\mathbf{t}_i \\ d_i^{\lambda}\mathbf{r}_i\times\mathbf{n}_i & \dot{d}_i\mathbf{r}_i\times\mathbf{n}_i & d_i^{\lambda}\mathbf{r}_i\times\mathbf{t}_i\end{bmatrix}\begin{bmatrix}k_i\\ c_i\\ k_i\mu_i\end{bmatrix} \\
&= \sum_{i=1}^{n}\mathbf{A}_i\mathbf{p}_i
\end{aligned} \tag{7}$$

or in a more compact form of

$$\mathbf{w} = \sum_{i=1}^{n}\mathbf{A}_i\mathbf{p}_i = \mathbf{A}\mathbf{p} \tag{8}$$

In the above equation,

$$\mathbf{w} \equiv \begin{bmatrix} \mathbf{f}_c \\ \mathbf{m}_c \end{bmatrix}$$
$$\mathbf{A} \equiv \begin{bmatrix} \mathbf{A}_1 & \mathbf{A}_2 & \cdots & \mathbf{A}_n \end{bmatrix} \tag{9}$$
$$\mathbf{p} \equiv \begin{bmatrix} \mathbf{p}_1 \\ \mathbf{p}_2 \\ \vdots \\ \mathbf{p}_n \end{bmatrix}$$

and

$$\mathbf{A}_i \equiv \begin{bmatrix} d_i^{\lambda}\mathbf{n}_i & \dot{d}_i\mathbf{n}_i & d_i^{\lambda}\mathbf{t}_i \\ d_i^{\lambda}\mathbf{r}_i \times \mathbf{n}_i & \dot{d}_i\mathbf{r}_i \times \mathbf{n}_i & d_i^{\lambda}\mathbf{r}_i \times \mathbf{t}_i \end{bmatrix}$$
$$\mathbf{p}_i \equiv \begin{bmatrix} k_i \\ c_i \\ k_i\mu_i \end{bmatrix}, \quad i = 1, 2, \cdots, n \tag{10}$$

In relation (8), the 6-dimensional vector w is the resultant contact wrench (consisting of the resultant contact force and moment) about a fixed reference point on the contact body and thus, can be measured by a 6-axis force-moment sensor attached to this reference point. The 6×3n matrix A defines the kinematic relations between the said reference point and the n individual contact points, which can be computed based on the known geometry of the contact body and the measured relative motion between the two contact bodies, namely, $(\mathbf{x}, \boldsymbol{\theta})$. The parameter vector $\mathbf{p}$ comprises the 3n model parameters which are unknowns in the model identification problem.

It is clear from (9) and (10) that the resultant contact wrench w can be measured and the coefficient matrix A can be computed if the kinematics and motion states of the two contact bodies are known. However, relation (8) is insufficient for uniquely defining the unknown parameter vector $\mathbf{p}$ in terms of the measured w and computed A, because the system has only 6 equations and 3n unknowns, even for single-point contact case where $n = 1$ because the coefficient matrix A is rank-deficient. To simplify the problem, an assumption can be made as originally specified in (Weber, Ma, and Sharf 2006). This is to assume that each contact body has the same contact parameters everywhere around its body, namely, $\mathbf{p}_1 = \cdots = \mathbf{p}_n = \overline{\mathbf{p}}$ in (8). It should be emphasized that such an assumption is not unpractical because engineers usually assume each contact body having the same contact stiffness, damping, and friction properties everywhere around the body. If a body does have different parameter values in different locations, say, for example, two different friction coefficients in two separate faces, this body can then be partitioned into two sub-bodies with each different frictional face being inclusively included in one sub-body. With the assumption of $\mathbf{p}_1 = \cdots = \mathbf{p}_n = \overline{\mathbf{p}}$, equation (8) is reduced to

$$\mathbf{w} = \left(\sum_{i=1}^{n} \mathbf{A}_i \right) \overline{\mathbf{p}} = \mathbf{A}\overline{\mathbf{p}} \tag{11}$$

where **w** remains unchanged as defined in (9) but **A** and **p** become

$$\mathbf{A} = \begin{bmatrix} \sum_{i=1}^{n} d_i^{\lambda}\mathbf{n}_i & \sum_{i=1}^{n} \dot{d}_i\mathbf{n}_i & \sum_{i=1}^{n} d_i^{\lambda}\mathbf{t}_i \\ \sum_{i=1}^{n} d_i^{\lambda}\mathbf{r}_i \times \mathbf{n}_i & \sum_{i=1}^{n} \dot{d}_i\mathbf{r}_i \times \mathbf{n}_i & \sum_{i=1}^{n} d_i^{\lambda}\mathbf{r}_i \times \mathbf{t}_i \end{bmatrix} \qquad (12)$$

$$\overline{\mathbf{p}} = \begin{bmatrix} k \\ c \\ k\mu \end{bmatrix}$$

Now the dimensions of the coefficient matrix A and parameter vector **p** are reduced to only 6×3 and 3×1, respectively. This latter relation will serve as the basic relation for the identification procedure.

2.2.2 Identification Procedure

The identification method works, as formulated in Section 3.A, based on the following basic conditions:

(a) the position and orientation of each contact body, namely, $\mathbf{x}$ and $\boldsymbol{\theta}$, can be measured;

(b) the linear and angular velocities of each contact body, namely, $\dot{\mathbf{x}}$ and $\boldsymbol{\omega}$, can be measured;

(c) the resultant contact wrench (i.e., both the force and moment), namely, **w**, can be measured; and

(d) the geometry of the contact bodies is known.

The data in above items (a) and (b), namely, the position and orientation, velocity of a contact body, can be extracted from the measurement data collected by a 3D motion sensing system. The data in item (c), namely, the resultant contact wrench of each body, can be measured by a 6-axis force-moment sensor. The data in (d), namely, the geometry data, is described by the geometric parameters of the bounding surfaces of the contact bodies. They are available either from the CAD design or from the geometric measurement of the real hardware. These geometric parameters are assumed to be constant when they are expressed in the coordinate frames attached to their associated contact bodies.

With a single measurement of contact resultant wrench w and contact body's position-orientation x, one still cannot find the parameter vector p from relation (11) although the linear system has more equations than unknowns because matrix A is still rank-deficient in theory (the first two columns are linearly dependent). However, this problem disappears if two or more measurements are made unless all these measurements are obtained at the same pose without moving the contact body. In general, one can perform a sequence of m measurements, i.e., $(\mathbf{w})_1, (\mathbf{w})_2, \cdots, (\mathbf{w})_m$ and $(\mathbf{x}, \boldsymbol{\theta})_1, (\mathbf{x}, \boldsymbol{\theta})_2, \cdots, (\mathbf{x}, \boldsymbol{\theta})_m$ along a motion trajectory over a period of time. This will lead to a total of *m* sets of relation (11), which can be assembled into the following regression form

$$\mathbf{w} \equiv \begin{bmatrix} (\mathbf{w})_1 \\ (\mathbf{w})_2 \\ \vdots \\ (\mathbf{w})_m \end{bmatrix} = \begin{bmatrix} (\mathbf{A})_1 \\ (\mathbf{A})_2 \\ \vdots \\ (\mathbf{A})_m \end{bmatrix} \overline{\mathbf{p}} \equiv \mathbf{B}\overline{\mathbf{p}} \qquad (13)$$

where the augmented matrix **B** is defined as

$$\mathbf{B} \equiv \begin{bmatrix} (\mathbf{A})_1^T & (\mathbf{A})_2^T & \cdots & (\mathbf{A})_m^T \end{bmatrix}^T \qquad (14)$$

Equation (13) is a system of linear equations having a total of 6m equations and only 3 unknowns. It represents a standard linear identification problem, and thus, can be solved using least-square approximation as follows

$$\bar{\mathbf{p}} = (\mathbf{B}^T\mathbf{B})^{-1}\mathbf{B}^T\mathbf{w} \tag{15}$$

After vector $\bar{\mathbf{p}}$ is computed, the three individual contact parameters k, c, and μ can be readily obtained from the definition of $\bar{\mathbf{p}}$ in (12). Pre-process of measured raw data can be performed to render matrix A better-conditioned numerically and special factorization techniques like Household-reflection method may be used to evaluate the right-hand side of equation (15) for better numerical results. Alternatively, starting from the second measurements (i.e., $m \geq 2$), equation (13) can be solved for $\bar{\mathbf{p}}$ at any instant along with the measurement by using the recursive least-square method to provide a time history of the estimated results. This alternative will be very useful for real-time model update in the application of adaptive control of contact motions.

The above-mentioned identification procedure is illustrated in a diagram shown below:

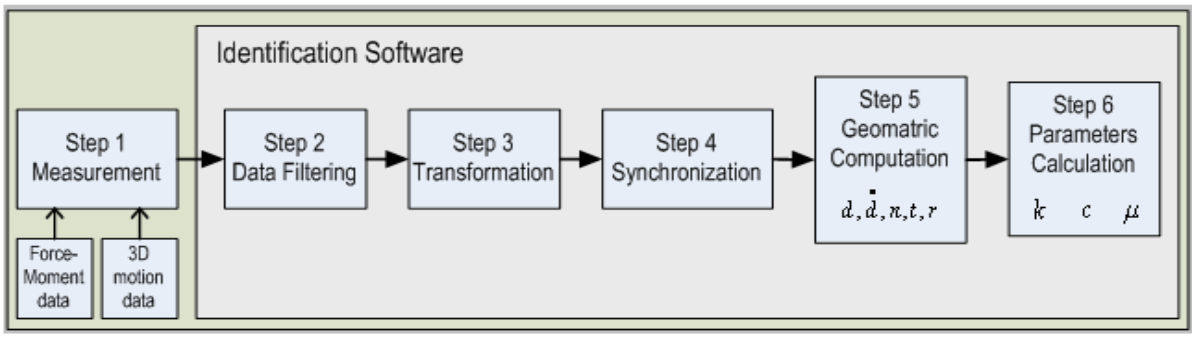

3. EXPERIMENT TESTBED

In order to experimentally study and verify the parameter identification method described in Sections 2.2.2 and 2.2.3, one needs to design and build an experiment system which can generate multiple-point contact in a predictable manner. Based upon the identification procedure, the experiment system must be capable of measuring the 3D position, orientation, velocities and resultant contact wrench of each of the two contact bodies. Obviously, a 6-DOF robotic arm is an ideal device for this purpose because a robot can provide a controllable 3D motion to a rigid body. With this consideration, a robotics assisted experiment testbed was designed. The system and its working principle are conceptually shown in Fig.4.

In order to conduct the intended experimental verification of the parameter identification method, the test system must meet a number of basic requirements. These requirements and how they are met by this test system are outlined below.

1) The system should be capable of providing general and also repeatable 3-D contact motions.

   A 6–DOF Staubli RX90L robot is employed. The robot can be programmed to provide a repeatable 3-D motion for the tested contact object at an accuracy level of 0.1 mm.

2) The system should be capable of measuring the resultant contact force and moment of at least one of the two contact bodies in all three axes.

   This requirement is met by installing a 6-axis force-moment sensor in the bottom of the fixed contact body (see Figs. 5&6). The 6-axis ATI Omega160 force-moment sensor has enough load capacity and frequency bandwidth to catch the force signal of small impact (large impact is out of scope of this research because of the assumption of low-speed impact) at a sampling rate of over 1000 Hz.

3) The system should be capable of accurately measuring the 3-D position and orientation of each of the two contact bodies in all three axes.

   Measuring the position and orientation of a contact body in 3-D is difficult because the body can move arbitrarily in all axes during a contact motion. An NDI's Optotrak infrared-based 3-D motion

sensor is used to perform this task. This sensor can track the positions of up to 24 active marks attached to the contact body at a resolution of 0.1 mm within a volume of 2×2×1 meters and a sampling rate of 450~3500Hz depending on the number of markers used in the measurement. The sensor system is shown in Fig.5 and some of the markers are shown in Fig.6.

4) The system should be capable of obtaining the 3-D linear and angular velocities of each contact body due to the formulation related to the contact damping and friction.

   Direct measurement of 3-D velocity is difficult. The required velocity data are derived from differentiating and filtering the position and orientation data. It may also be obtained by integrating the accelerometer data, which may generate smoother velocity data but accelerometers are required. So far, velocities have been obtained from differentiation only. The result is satisfactory because the tests involved only very slow contact motions.

5) The system should be capable of synchronizing the measurements specified from 2) to 4) because all the motion and force data for each equation must measured at the same time.

   The Labview software is used to trigger and coordinate the data acquisition processes of all the individual sensor units in the system so that the same time will be stamped on all the sensors data.

6) The contact interfaces should be capable of producing multiple contacts in a predictable fashion because the tested identification is for multi-point contact cases.

   A basic prototype of an H-shaped peg and a square mating hole have been built, as shown in Fig.6. The square hole actually consists of four separately adjustable side plates and a bottom plate. Such a pair of contact bodies can generate from one to five simultaneous contact points by maneuvering the pose of the peg with respect to the hole. The location of each contact point is predictable.

7) The geometry models of contact bodies should be known because the identification method requires predicting the locations of all the contact points.

   Due to their relatively simple geometries, the surfaces of the H-peg and the square hole (comprising the inner surfaces of the five plates) can be accurately measured and modeled in the computer. With such a geometry or kinematics model, the locations of all the contact points between the peg and the hole can always be precisely computed as long as the relative position and orientation between the peg and hole are known.

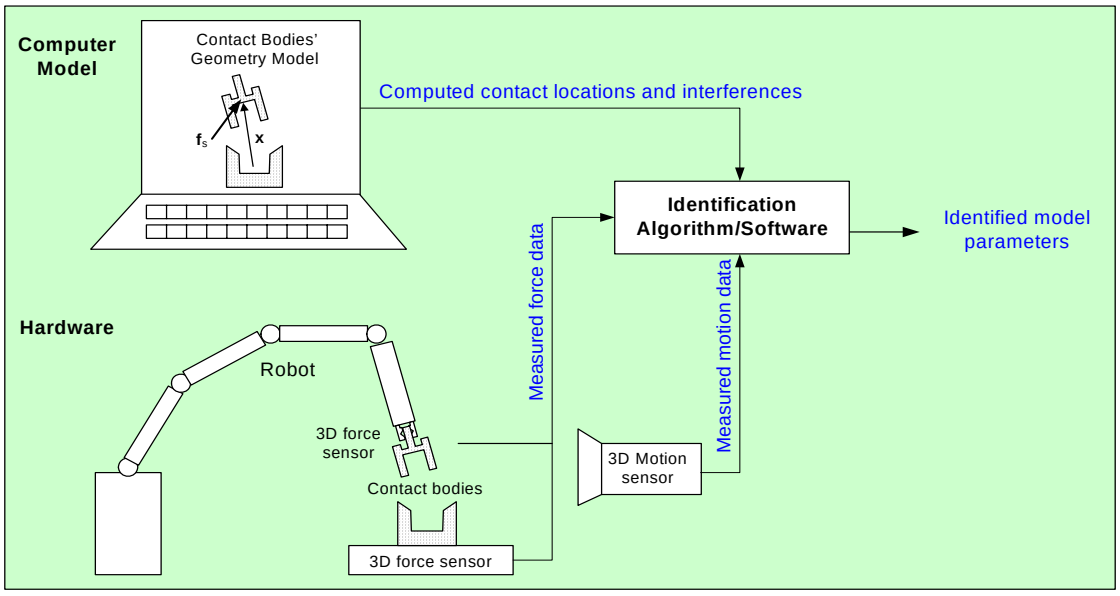

Figure 4. Concept of the experiment system for testing the identification method

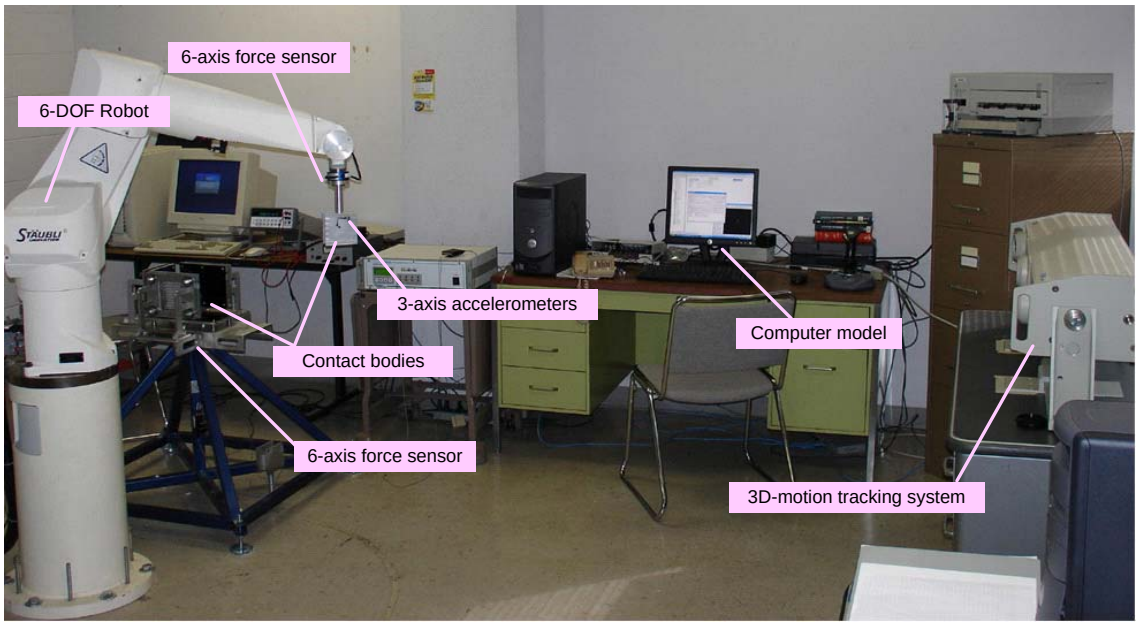

Figure 5. Integrated hardware system of the contact parameter identification experiment testbed

The H-shaped peg is made of aluminum and the contact plates are made of steel with special surface treatments for having sustainable friction and anti-scratch properties. Each plate (or wall) of the square hole is supported by a set of four linear bearings with springs so that the plate can linearly move along its normal direction when it is subject to a contact force and restore its original position when the contact force is gone. The stiffness's and locations of the four springs (which are symmetrically distributed) determine a compound stiffness at any given contact point on the plate. This compound stiffness is used to represent the contact stiffness of the peg-plate contact dynamics model. Similarly, the deflections of the four springs can be used to determine the deflection at the contact point. Since the spring is much softer than the materials of the peg and plate, the real material stiffness's of the peg and plate can be ignored (otherwise they are too difficult to deal with because their associated suffice deflections are too small to be physically measured by the currently available sensors in the lab). It should be pointed out that the compound stiffness varies nonlinearly with respect to the location of the contact point. This non-constant stiffness value is undesirable for the purpose of the experiment. However, it can be shown that, if the contact point moves within a small area around the center of the plate (say, in an area with a radius of no more than 5% of the distance between two springs), the compound stiffness is approximately a constant (with an error of less than 1%). The compound stiffness value can be calculated as

$$k = \frac{4(k_2k_3k_4 + k_1k_3k_4 + k_1k_2k_4 + k_1k_2k_3)}{(k_1 + k_3)(k_2 + k_4)} \tag{16}$$

where k_i is the stiffness of the ith spring ($i = 1,2,3,4$). Obviously, if all the four springs have the same stiffness value, then the compound stiffness is simply the sum of all the four stuffness values.

So far, no special damping devices have been installed in the contact hardware and thus, the identified damping parameters reflect the real contact damping between the two contact objects.

It should be pointed out that the true stiffness value can be easily measured statically using a force gauge and a potentiometer, which was what we did on the project. On the contrary, the true value of a contact damping parameter is very difficult to measure. We have not done an independent measurement of the true damping parameters but we are intended to do it in the future.

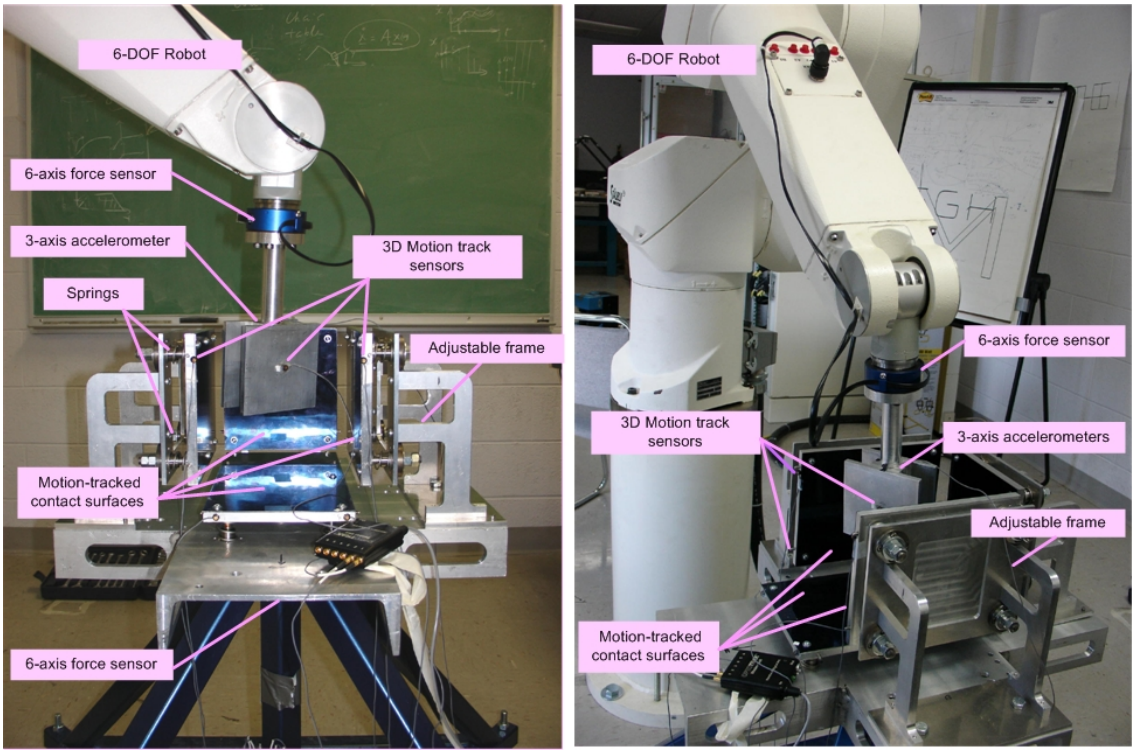

Figure 6. The instrumented contact interfaces of the experiment testbed

In the system, one of the two contact bodies is attached to a grounded base through a 6-axis force-moment sensor. In such a way, this body is fixed to the ground and thus, its absolute motion can be assumed always zero. The other contact body is grasped and manipulated by a 6-DOF robotic arm. Thus, the absolute motion of the second body is equal to the relative motion between the two contact bodies. Using the robot, the 3D motion of the moving body (i.e., the relative motion between the two contact bodies) can be precisely controlled in order to generate predictable multiple contacts between the two contact bodies. Although the motion (i.e., the pose and velocities) of the movable contact body can be computed by the forward kinematics of the robotic arm from its known joint trajectories, it is still independently measured by an external motion sensor for better accuracy. The resultant contact wrench exerted on the fixed contact body is measured by a 6-axis force-mention sensor installed in the bottom of the body and that exerted on the moving contact body is measured by another 6-axis force-moment sensor installed in the wrist of the robotic arm. The measured motion and force data are fed into the identification software as the input data for identifying the contact parameters. The contact geometry model in the computer is used to compute the detailed locations and geometric interferences (for approximating the surface deflections) of all the simultaneous contact points. This geometric computation is part of the identification procedure being carried out inside the identification software. The output of the identification software is a set of identified contact model parameters.

All the hardware components and some of the software components had been designed and developed prior to this project. The hardware integration had also been completed prior to this project. The software implementation and integration were mostly done by this project. So far, the complete hardware and software system has been tested only with single-point contact and two-point contact cases. More software implementation work is still needed for handling more complicated multiple-point contact cases and thus, this part of the work has to be done beyond this project in the near future. A few different views of the integrated hardware system are shown in Figs.5&6.

4. TEST RESULTS

In order to facilitate the investigation, we planned to perform our tests incrementally from simple cases to complicated cases. We started our test with a single-point contact case and then moved to a two-point contact case. Due to the time limitations of this short-term project, we could only do the single-point and two-point contact cases. The test results of these two basic cases are described in the next two subsections.

4.1 Single-Point Contact Tests

The hardware setup of the single-point contact test is shown in Fig.7. In the test, the robotic arm is commanded to move rod-like contact object along a predefined trajectory to make contact with the bottom plate of the testbed. The position and contact force data are collected by the motion and force sensors during the test for identification purpose. Such a test is done repeatedly for many times in order to obtain better statistical results. A typical motion path of the contact object sensed for a test is shown in Fig.8. The time histories of the measured contact force and moment for the same test are shown in Figs.9 and 10. The deflection of the contact point and its time rate which are computed from the time history of the position data are shown in Fig.11. Matlab's "filter" function has been used to smoothen the results in the computation of d and $\dot{d}$. Fig.12 shows the normal contact force versus the contact deflection where we can clearly see the hysteresis caused by the contact damping.

As an example, the identified parameter values from a set of seven tests are listed in Table 1. In each test, measurements are taken at about 150 points along the motion trajectory (within the contact period of the trajectory only), namely, $m = 150$ in equation (13). As one can see, the average value of the identified contact stiffness is only 2.1% off its true value. The true stiffness values were obtained by separate manual measurements. Unfortunately, the true values of the damping and friction parameters are very difficult to obtain and thus, they were not available yet for measuring the absolute identification errors. For now, we use the standard deviation (STD) of a series of tests to statistically measure the relative identification errors. The standard deviations among the seven listed tests are 2.7%, 6.1% and 4.3%, respectively, for the identified stiffness, damping, and sliding friction parameters. This kind of accuracy level is indeed quite good from a practical point of view.

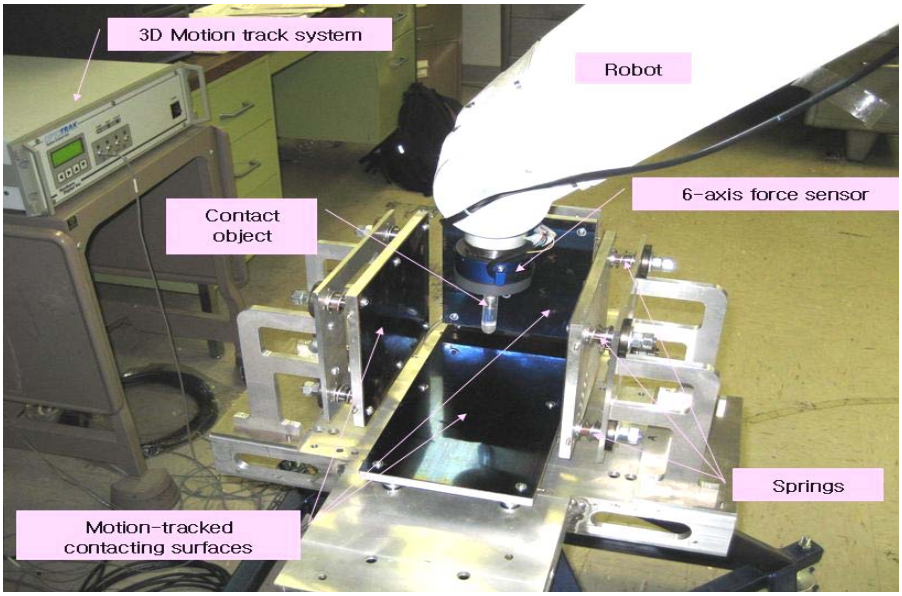

Figure 7. Hardware setup for single-point contact test

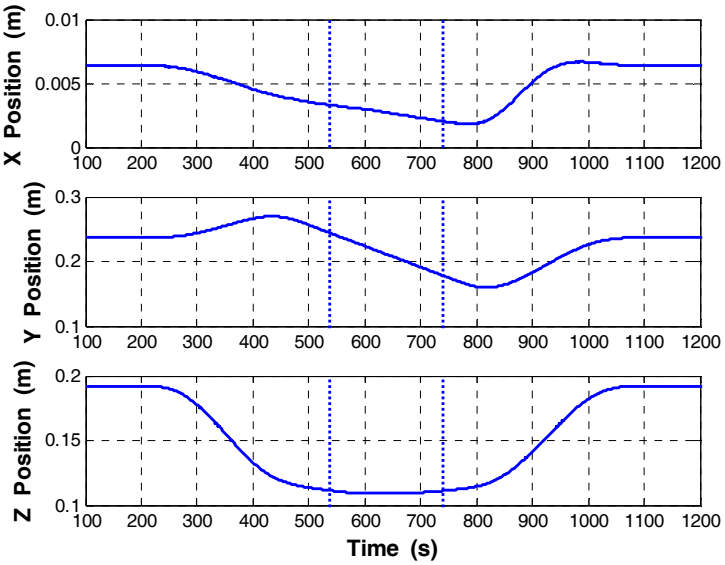

Figure 8. Motion trajectory of the contact body handled by the robot (contacting period is between the two dashed lines)

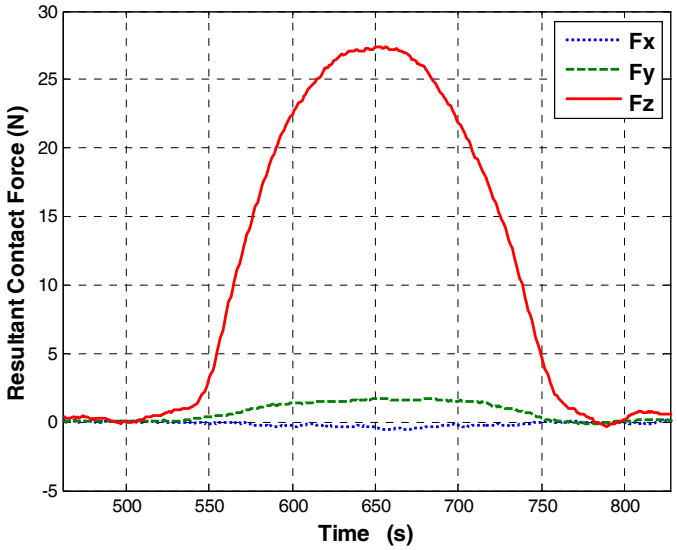

Figure 9. Resultant contact force

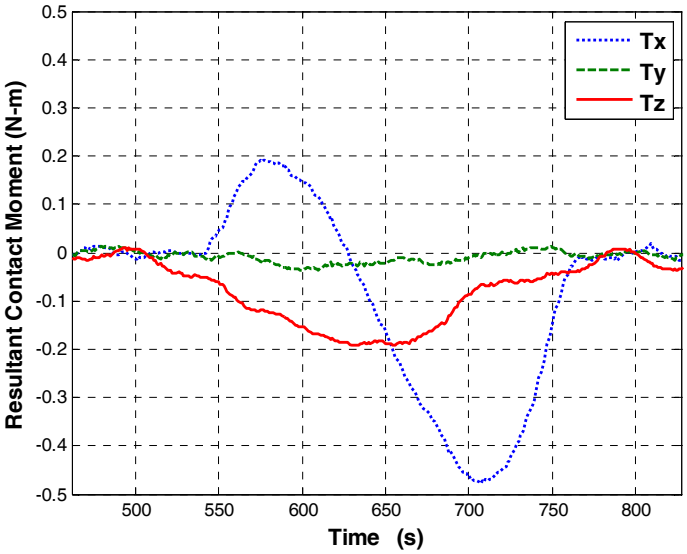

Figure 10. Resultant contact moment

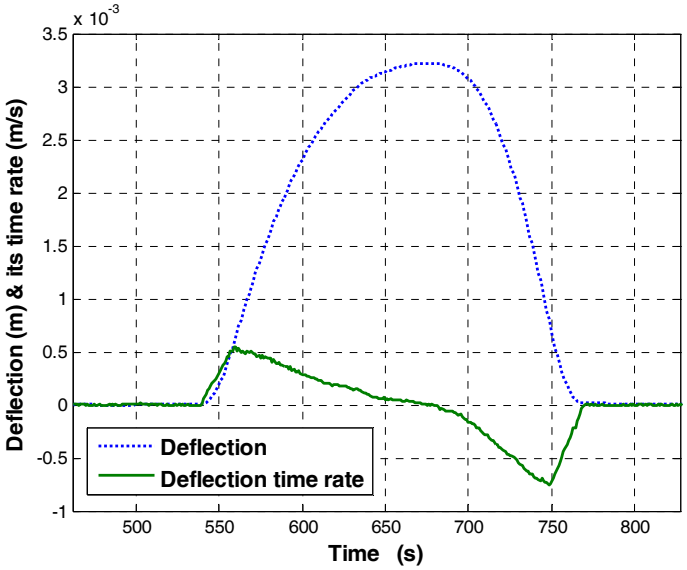

Figure 11. Contact deflection and its time derivative

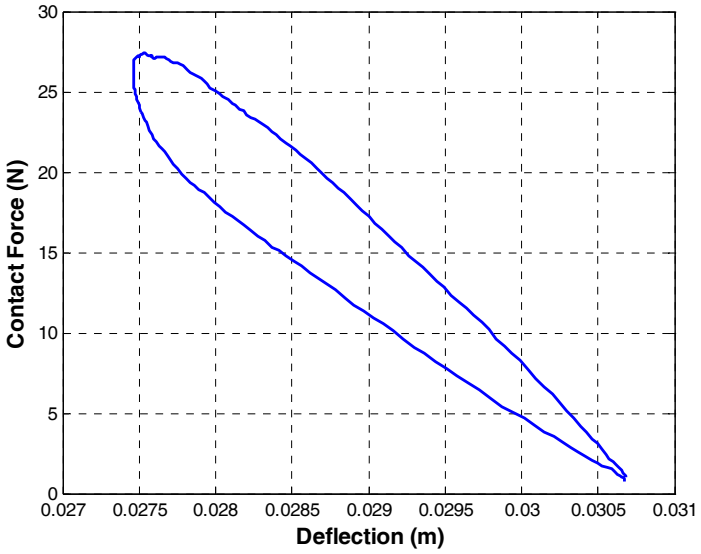

Figure 12. Contact force versus deflection at the contact point

Note from Table 1 that the identification error of stiffness measurement is less than these of damping and friction measurements. This is mainly because the relative motion speeds between the contact bodies in these tests were relatively low. From the formulation presented in Section 3, one can easily understand that stiffness parameters can be identified statically while damping and sliding friction parameters have to be identified with nonzero velocity. When the relative speed between the contacting bodies is low, the measured motion data will have low signal-to-noise ratio and thus leads to more errors in identified damping and friction parameters. Also, the sliding friction model is no longer representative at very low speed.

Table 1 Identified contact parameters and their errors

Parameters	$k\ (N/m)$	$c\ (Ns/m)$	μ
Error[2]	**2.1%**	**N/A**	**N/A**
STD	**2.7%**	**6.1%**	**4.3%**
Average	**8389.6**	**5299.6**	**0.0652**
Test 1	8456.2	5461.60	0.0620
Test 2	8426.7	5871.20	0.0652
Test 3	8316.2	5537.10	0.0649
Test 4	8635.9	4838.90	0.0623
Test 5	7889.5	5252.60	0.0711
Test 6	8391.5	5048.20	0.0658
Test 7	8611.3	5087.50	0.0649

[2] Absolute error compared to the true value of the parameter.

It has been observed in many different tests that increasing the contact motion speed can improve the identification results for the damping and sliding-friction parameters but it also reduces the accuracy of stiffness identification. Such a result is understandable because the damping and sliding-friction must be measured in a dynamic condition but the stiffness is better measured in a static condition. This makes it challenging to simultaneously identify all the three different types of parameters. We will be developing techniques to deal with this problem as well as the problem of identifying the difficult static-friction parameters in an on-going research.

4.2 Two-Point Contact Tests

The hardware setup of a two-point contact case is shown in Fig.13. In the test, the H-peg was moved by the robot to contact the side plate first (single-point contact) and then slide down until one corner of the peg touches the bottom plate (two-point contact). The peg will then continue to move while peeking contact in two points. As we can see from Fig.14, the two simultaneous contact points are located on two different contact bodies (i.e., the two plates).

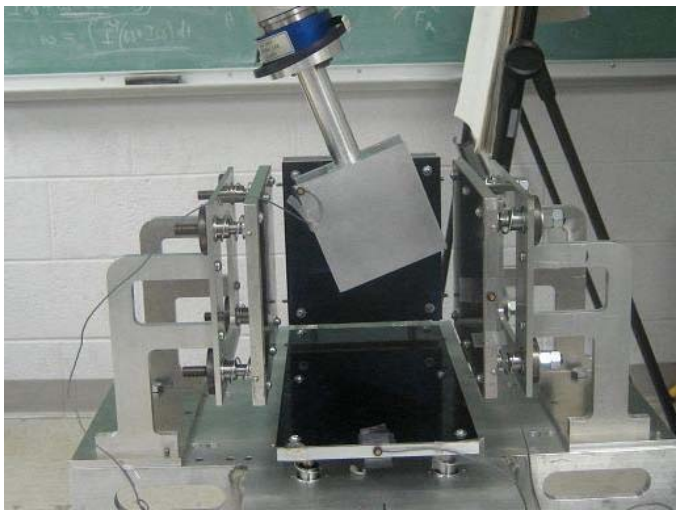

Figure 13. Contact interface hardware for two-point contact test

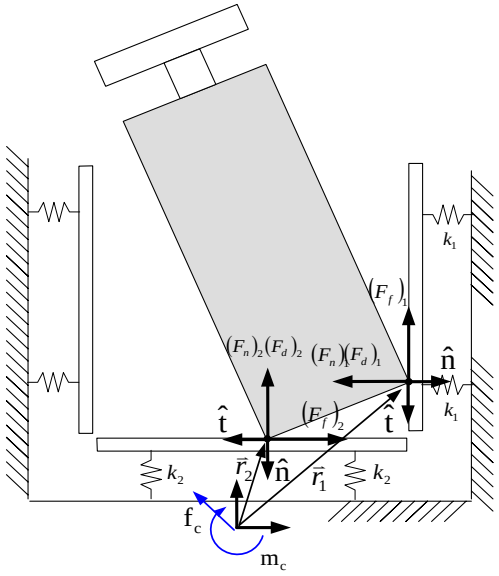

Figure 14. The two contact points of the two-point contact case

Since the two contact points are on two different bodies (one on the side plate and the other on the bottom plate) and they have different contact properties, there are two sets of unknown contact parameters to be identified in this case. The material properties of all springs and plates, such as the stiffness coefficient , are assumed to be identical. However, in a pre-test, the spring constant of the vertical contact wall (after assembly) was found higher than its manually-measured stiffness of the springs. Thus, the model of the contact scenario had to be modified with stiffer spring constant for the vertical contact wall. The source of stiffer spring constant is the additional friction force caused by the self weight of the vertical contact surface. Thus, equation (13) has to be modified with two sets of different model parameters, which yields the following force relations:

$$\begin{aligned} F_{Total} &= -k_1 d_1 \hat{n}_1 - c_1 \dot{d}_1 \hat{n}_1 - \mu_1 k_1 d_1 \hat{t}_1 - k_2 d_2 \hat{n}_2 - c_2 \dot{d}_2 \hat{n}_2 - \mu_2 k_2 d_2 \hat{t}_2 \\ M_{Total} &= -k_1 d_1 \vec{r}_1 \times \hat{n}_1 - c_1 \dot{d}_1 \vec{r}_1 \times \hat{n}_1 - \mu_1 k_1 d_1 \vec{r}_1 \times \hat{t}_1 - k_2 d_2 \vec{r}_2 \times \hat{n}_2 - c_2 \dot{d}_2 \vec{r}_2 \times \hat{n}_2 - \mu_2 k_2 d_2 \vec{r}_2 \times \hat{t}_2 \end{aligned} \tag{17}$$

This relation can be written into the following matrix form

$$\overline{W} \equiv \begin{bmatrix} W_1 \\ W_2 \\ \vdots \\ W_m \end{bmatrix} = \begin{bmatrix} A_1 \\ A_2 \\ \vdots \\ A_m \end{bmatrix} \overline{P} \equiv B\overline{P} \tag{18}$$

where

$$W_i = \begin{bmatrix} F_{xi} \\ F_{yi} \\ F_{zi} \\ M_{xi} \\ M_{yi} \\ M_{zi} \end{bmatrix}, \quad \overline{P} = \begin{bmatrix} k_1 \\ c_1 \\ \mu_1 k_1 \\ k_2 \\ c_2 \\ \mu_2 k_2 \end{bmatrix} \tag{19}$$

$$A_i = \begin{bmatrix} -d_{1i} & -\dot{d}_{1i} & 0 & 0 & 0 & d_{2i} \\ 0 & 0 & 0 & 0 & 0 & 0 \\ 0 & 0 & d_{1i} & d_{2i} & \dot{d}_{2i} & 0 \\ 0 & 0 & d_{1i}(r_y)_{1i} & d_{2i}(r_y)_{2i} & \dot{d}_{2i}(r_y)_{2i} & 0 \\ -d_{1i}(r_z)_{1i} & -\dot{d}_{1i}(r_z)_{1i} & -d_{1i}(r_x)_{1i} & -d_{2i}(r_x)_{2i} & -\dot{d}_{2i}(r_x)_{2i} & d_{2i}(r_z)_{2i} \\ d_{1i}(r_y)_{1i} & \dot{d}_{1i}(r_y)_{1i} & 0 & 0 & 0 & -d_{2i}(r_y)_{2i} \end{bmatrix} \tag{20}$$

Equation (18) can be solved using least-square approximation as follows

$$\overline{P} = \left(B^T B\right)^{-1} B^T \overline{W} \tag{21}$$

Measured test data of the two-point contact case are plotted in Fig.15 though Fig.21.

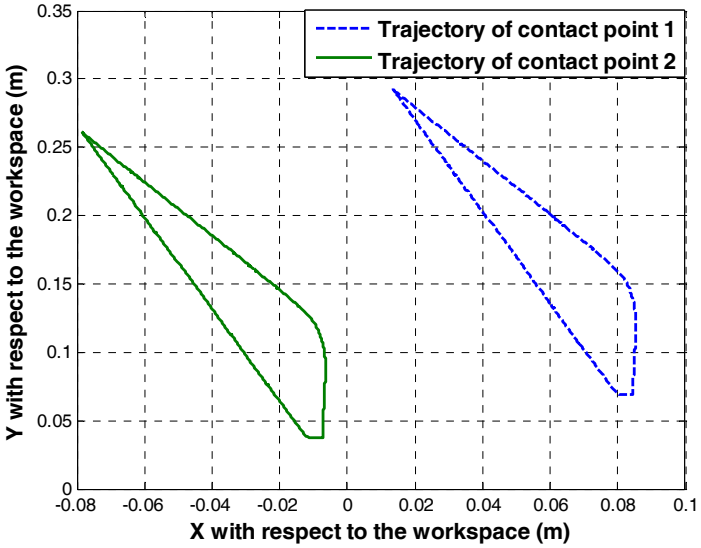

Fig. 15 Motion trajectory for two-point test with respect to the workspace (X and Y are in horizontal and vertical directions, respectively)

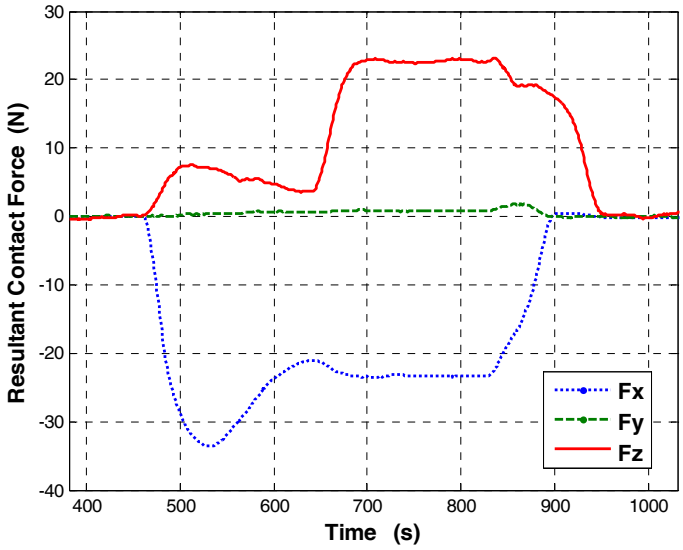

Fig. 16 Resultant contact force measured from the two-point contact test

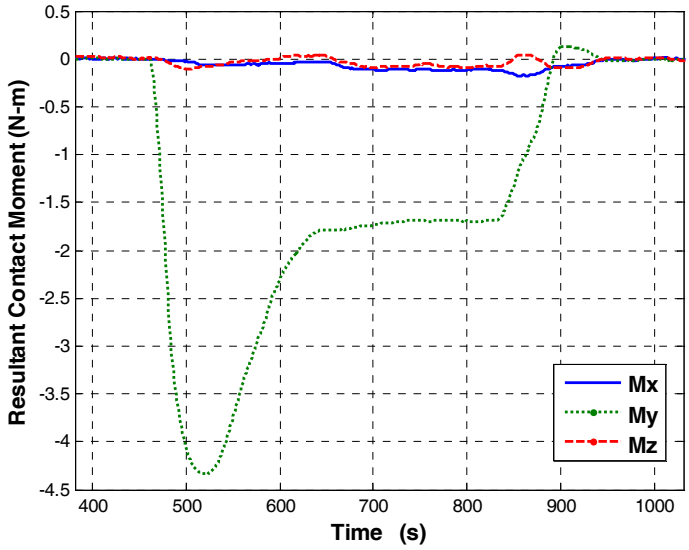

Fig. 17 Resultant contact moment measured from the two-point contact test

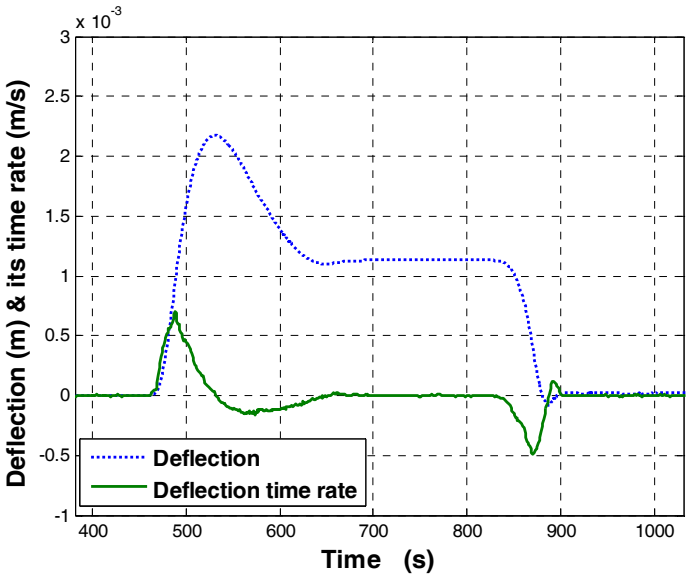

Fig.18 Contact deflection and its time derivative of the first contact point

(It occurs on the right-hand side plate)

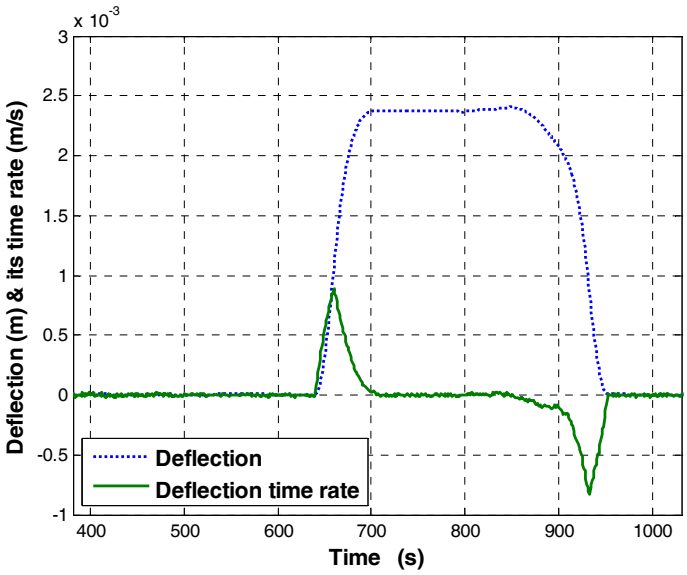

Fig. 19 Contact deflection and its time derivative of the second contact point (It occurs on the bottom plate)

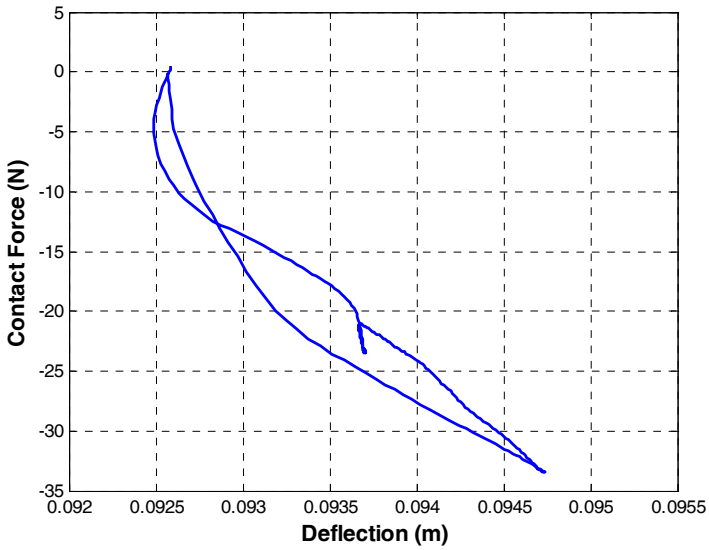

Fig. 20 Contact force versus deflection associated with the first contact point

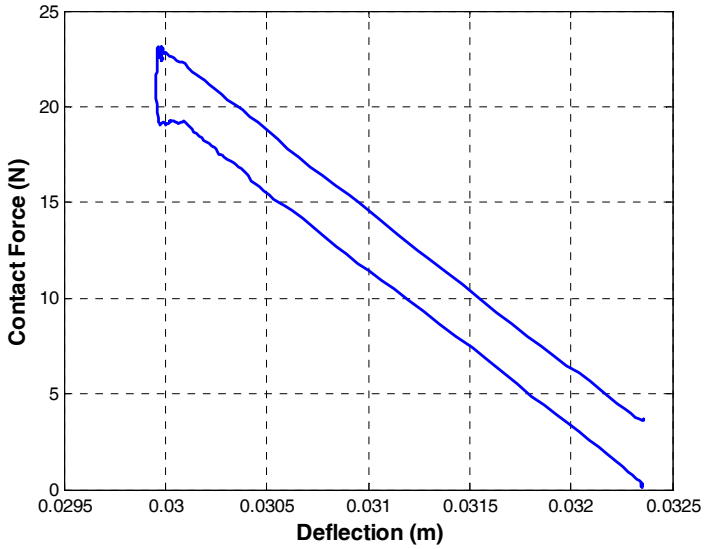

Fig. 21 Contact force versus deflection associated with the second contact point

Based on a number of repeated tests of the two-point test case and using the modified identification procedure described in equation (18), we identified the six unknown parameters, as listed in Table 2.

The standard deviations of the identified stiffness, damping, and friction parameters from different test groups vary in the ranges of 2%~3%, 15%~25% and 5%~7%, respectively. The higher ends of the error ranges are always associated with the parameters of the first contact point and the lower ends of the error ranges are with the second contact point. The error levels for the stiffness and friction parameters may be acceptable in practice but the error level for the damping parameter is too high.

Table 2 Identified contact parameters from two-point contact case

Parameters	$k_1(N/m)$	$c_1(Ns/m)$	μ_1	$k_2(N/m)$	$c_2(Ns/m)$	μ_2
Error	**2.9%**	**N/A**	**1.9%**	**4.8%**	**N/A**	**18.6%**
σ	**3.1%**	**15.1%**	**5.7%**	**2.4%**	**25.2%**	**7.3%**
Average	**15109.25**	**5541.40**	**0.2086**	**7509.35**	**329.44**	**0.2613**
Test1	**15394.00**	**5691.30**	**0.2012**	**7385.20**	**238.09**	**0.2408**
Test2	**15406.00**	**5370.20**	**0.1826**	**7408.20**	**332.17**	**0.2995**
Test3	**15557.00**	**4084.10**	**0.2242**	**7872.20**	**452.85**	**0.2709**
Test4	**15374.00**	**4244.60**	**0.2074**	**7238.60**	**311.61**	**0.2383**
Test5	**15248.00**	**6106.00**	**0.2115**	**7475.40**	**242.24**	**0.2626**
Test6	**15295.00**	**5960.00**	**0.2080**	**7470.50**	**456.10**	**0.2437**
Test7	**14334.00**	**6453.80**	**0.2130**	**7654.90**	**382.48**	**0.2638**
Test8	**14266.00**	**6421.20**	**0.2206**	**7569.80**	**220.00**	**0.2710**

An investigation of the error sources revealed that the unmodeled friction and backlash in the linear bearings of the vertical plate are the major attributing factors to the errors. This problem can be solved by

using a lighter plate and smoother linear bearings for the vertical plate but the testing hardware has to be redesigned. It can also be compensated in the identification model but the unmodelled factors have to be first identified. We have not done either of these two correction measures because: 1) we did not have enough time for the short project and 2) these errors are caused by the imperfection of the testbed rather than the identification method itself.

Another possible error source is the unmodelled static friction in contact testing. Since part of the contact motion involves sticking and the static friction is not factored into the identification algorithm, the effect of the static friction must have been reflected in the identified parameters. Because the static friction is a nonlinear phenomenon, it is a very difficult task to identify the static friction parameter(s) in the identification procedure. It requires further research work to include the static friction in the identification method.

5. CONCLUSIONS AND DISCUSSIONS

5.1 Conclusion of the Project

A uniquely designed, robotics-based experimental testbed was used to test a systematic method of identifying contact-dynamics model parameters. The tested identification method is capable of simultaneously identifying the key stiffness, damping, and friction parameters of a general contact-dynamics model directly from hardware test of a pair of contact objects which can have complicated geometries and multi-point frictional contacts. The identification method can also be used to extract contact-dynamics model parameters of a dynamic system from routine tests of its contact hardware. Although having been proposed and studied earlier, the method had never been experimentally verified before this project. The method cannot be accepted by the industry for practical use without being experimentally verified. This project served this purpose.

In this project, single-point contact and two-point contact cases are tested. The results of the single-point test demonstrated very good accuracy, whose identification errors are 2.7%, 6.1% and 4.3% for the three identified parameters (i.e., the stiffness, damping and friction parameters), respectively. Considering many inevitable errors and uncertainties in the complicated nonlinear system, such an error level is acceptable in practice. However, the results of the two-point contact case showed higher errors than the single-point contact case. The identification errors in the three identified parameters associated with the first contact point are 3.1%, 15.6%, and 5.7% and these associated with the second contact point are 2.4%, 26.8%, and 7.3%, respectively. Obviously, the error in the damping parameter is high.

Investigation of the 2-point contact case revealed some of the possible error sources. Some of the error sources were due to different contact properties in the two different contact locations. Others are due to the design of the contact interface such that the parameters to be identified are affected by other factors in the devices (such as the friction inside the support bearings). Identification algorithm has been modified (as described in Section 4.2 to account for different parameter values in different contact locations. However, redesign of the contact interface hardware is impractical for this short-term project and thus, no action was made so far to correct contact-interface design problem. We will attach this problem in the future research.

Due to the time and funding limitations, testing of cases involving more than two contact points have not been done in this short project. However, this will be done in the future research.

5.2 Further Research

The identification method having been investigated so far was derived based on the following assumptions (conditions):

1) only sliding friction is considered (i.e., sliding friction condition)
2) the inertial force on the contact body is ignored (i.e., quasi-static condition)
3) the model parameters for every contact point of the same contact body are the same (i.e., isotropy condition)

These assumptions help focus the identification problem on a more understandable and fundamental level, from which a feasible solution procedure can be derived and experimentally tested. As learned from industrial practice, these assumptions are also reasonable approximations for modelling and simulation practice in industry. Therefore, this proposed short-term research project will focus on experimental verification of the identification method under these assumptions. This first step will pave the necessary pace for more advanced research where the above mentioned assumptions are removed.

Understandably, the parameters being identified based on these assumptions may have non-negligible errors for application cases violating these assumptions. Therefore, for more accurate modelling and simulation of future dynamic systems with contact motions, it is desirable to study how to deal with the situations without these assumptions. Since the removal of these assumptions will complicate the identification problem in both theory and experiment, further research are needed in the future. Since the research is quite fundamental and intensive, a research proposal will be submitted either to ARO or NSF in the future. The main topics to be addressed in the proposal are briefly described below for information purpose.

(1) <u>Contact involving both Static and Kinetic Frictions</u>

Many contact scenarios of a dynamic system in real life involve not only sliding friction but also static friction. Some even have more complicated friction situations such as skip-slip and jamming. A simulation model of such dynamic system must include not only sliding friction parameters but also static friction parameters. Thus, one needs to identify static friction parameters. An idea of how to include the static friction parameters in the method will be discussed here. Assume the bristle friction model described in eq.(4) is used and also assume all the contact parameters are unchanged from one contact point to another. Since static friction and sliding friction appear only one at a time for each contact point, one can introduce a switch function δ_i to switch between the two in the friction model. With this, equation (4) becomes

$$\mathbf{f}_{fi} = -(1-\delta_i)k_f \mathbf{s}_i - \delta_i k\mu d_i^{\lambda} \quad \text{where } \delta_i = \begin{cases} 0 & \text{if } |\mathbf{s}| < s_{\max} \quad \text{(sticking)} \\ 1 & \text{if } |\mathbf{s}| \geq s_{\max} \quad \text{(sliding)} \end{cases} \tag{22}$$

The switch function depends on the friction status which will be determined as a part of the algorithm computing the **A** matrix and the contact detection procedure as described in (Nahon 1994, Ma et al. 1997). Correspondingly, the coefficient matrix **A** and the parameter vector $\bar{\mathbf{p}}$ in relation (12) are now expanded to the following form

$$\mathbf{A} = \begin{bmatrix} \sum_{i=1}^{n} d_i^{\lambda}\mathbf{n}_i & \sum_{i=1}^{n} \dot{d}_i\mathbf{n}_i & \sum_{i=1}^{n} \delta_i d_i^{\lambda}\mathbf{t}_i & \sum_{i=1}^{n} (1-\delta_i)\mathbf{s}_i \\ \sum_{i=1}^{n} d_i^{\lambda}\mathbf{r}_i \times \mathbf{n}_i & \sum_{i=1}^{n} \dot{d}_i\mathbf{r}_i \times \mathbf{n}_i & \sum_{i=1}^{n} \delta_i d_i^{\lambda}\mathbf{r}_i \times \mathbf{t}_i & \sum_{i=1}^{n} (1-\delta_i)\mathbf{r}_i \times \mathbf{s}_i \end{bmatrix}, \quad \bar{\mathbf{p}} = \begin{bmatrix} k \\ c \\ k\mu \\ k_f \end{bmatrix} \tag{23}$$

As one can see, the additional parameter k_f for static friction is added to $\bar{\mathbf{p}}$ in the equation for identification. Now, one can use eq.(23) instead of eq.(12) in the identification procedure. The rest of the identification algorithm and procedure will remain the same.

(2) <u>Accounting for Inertia Forces (Transient Dynamics) in the Measurement</u>

If the contact body moves at a very slow speed during contact, the force and moment measured by each of the multi-axis force sensors as shown in Fig.4 may be considered as the resultant contact wrench

w of the associate contact body (assuming the gravity loading has been zeroed out in the sensor). However, when the relative speed between the two contacting bodies is not very low, the inertia force and moment (due to linear and angular accelerations) become significant and will be reflected in the sensor readings. This situation becomes significant during each impact period. In such a situation, the inertia force and moment can no longer be ignored. In other words, the transient dynamics needs to be considered.

To account for the inertia force in the identification formulation, one has to know the accelerations of the contact body. There are two ways of obtaining the accelerations of a contact body, one being to compute the accelerations from differentiating the measured position/orientation information and the other being to directly measure the accelerations of the contact body. Direct measurement of the accelerations is the better solution because differentiation of measured data will lead to poor numerical results.

With this consideration, the resultant contact wrench applied to equation (11) or (13) should be correspondingly modified to

$$\mathbf{w} = \mathbf{w}_{measued} - \mathbf{w}_{inertia} \tag{24}$$

where the inertia wrench $\mathbf{w}_{inertia}$ (with respect to the same reference point and frame as $\mathbf{w}_{measured}$) can be computed based one the known inertia properties, geometry information, and measured accelerations of the contact body.

(3) Non-constant Contact Model Parameters

If the contact parameters to be identified are assumed to vary continuously from point to point on the same contact body (e.g., $\overline{\mathbf{p}} = \overline{\mathbf{p}}(x, y, z)$), the problem will become extremely difficult to deal with. In such a case, eq.(13) alone is not enough to find even a discrete sets of $\overline{\mathbf{p}}(x, y, z)$ values at the corresponding contact points because matrix **A** is singular. Other conditions such as the known values of $\overline{\mathbf{p}}$ along the boundaries of each contact surface may have to be added for uniquely defined solution. Such a problem may have theoretical interest but will have little practical interest because currently nobody is modeling contact dynamics assuming its parameters being continuous functions of contact location.

Practically more interested case would be that the contact parameters are constant within each smooth surface (or face) but they vary from surface to surface (as opposed to varying from point to point). Since each contact body consists of a number of surfaces (e.g., a box-like body has 6 surfaces and a pyramid has four surfaces), there will be several sets of parameters to be identified, namely, $\overline{\mathbf{p}}_1, \overline{\mathbf{p}}_2, \cdots, \overline{\mathbf{p}}_m$ where the subscript represents surface number. The main formulation and procedure will remain the same as described in Section 2.2. However, the lower level formulation (not included in the proposal) will have to be extended to include a new layer to track the current contacting surfaces. This can be done because every contact point has been fully tracked in the kinematics computations of its location, velocity, and interference. Thus, the identification algorithm can switch parameter set from one to another when a contact surface changes. The largest difficulty in this problem is how to handle a contact point touching several surfaces (such as a contact occurs at a corner of a polyhedron) which involves different sets of contact parameters. One idea is to introduce a weighing factor for each involved surface to account for its contribution depending on the amount of the surface being involved in the contact region. Details of this approach need to be worked out in the future research.

(4) Optimal Test Trajectories

During identification procedure, the contact body can undergo different motion trajectories. Obviously, some of the trajectories will lead to more stable numerical process or more accurate parameter values than the others. For example, increasing motion speed will help identify damping parameters because damping parameters are sensitive to velocities. On the other hand, slowing down a contact motion will make static-friction parameters more identifiable because static friction forces present only

when the body is stationary or partially stationary. Moreover, since the kinematics matrix **A** depends on the configuration and velocity of the contacting body, its numerical condition will vary along different motion trajectories. As a result, the output of the numerical process of the identification procedure will also have different errors from one motion trajectory to another. Therefore, it is desirable to optimize the motion trajectories for experimental tests in order to get the best possible results. This is an interesting research topic useful not only for this identification project but also for nonlinear robot controls and operation optimizations.

(5) Software Toolkit

The real value of a new technology will not be realized until the technology is transferred to the end user, i.e., the ARL (Army Research Laboratories) or industry in this case. The logical next step of the research is to develop and validate an easy-to-use and reliable software tool for ARL. It is mostly desirable if such a toolkit is standalone or plug-in software toolkit to an existing simulation system. We envision that such an identification software toolkit can be developed in the future. Fig.22 illustrates how such an identification toolkit interfaces with an existing dynamic simulation system.

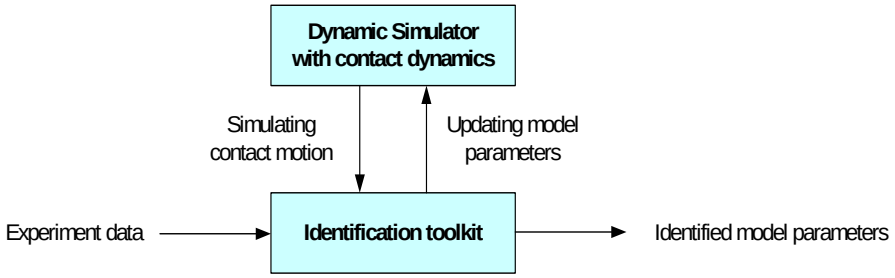

Figure. 22 An identification toolkit working with a multibody dynamics simulator

6. REFERENCES

[1] Agar, J., Sharf, I., Lange, C., and Gonthier, Y., 2005, “Contact parameter estimation with a space robot verification facility”, Proc. ASME Int. Design Eng. Tech. Confs. and Comp. and Info. in Eng. Conf., Long Beach, CA, pp. 433-442.

[2] Brach, R.M., 1991, Mechanical Impact Dynamics: Rigid Body Collision, John Wiley, NY.

[3] Erickson, D., Weber, M. and Sharf, I., 2003, “Contact Stiffness and Damping Estimation for Robotic Systems,” International Journal of Robotics Research, Vol. 22, No. 1, pp. 41-47.

[4] Gilardi, G. and Sharf, I., 2002, Literature survey of contact dynamics modeling, Mechanism and Machine Theory, Vol.37, No.10, pp.1213-1239.

[5] Gonthier, Y., McPhee, John; Lange, Christian; Piedboeuf, Jean-Claude, 2004, “A regularized contact model with asymmetric damping and dwell-time dependent friction”, Multibody System Dynamics, v 11, n 3, April, p 209-233.

[6] Goldsmith, W. Impact, 1960, Edward Arnold Ltd., London.

[7] Kraus, P.R. and Kumar V., 1996, Compliance contact models for rigid body collisions, Proc. IEEE Int. Conf. on Robotics and Auto., Albuquerque, NM, pp.1382-1387.

[8] Ma, O., Buhariwala, K., Roger, N., Maclean, J. and Carr, R., 1997, “MDSF — a generic development and simulation facility for flexible, complex robotic systems”, Robotica, Vol. 15, pp. 49-62.

[9] Ma O. and Boyden S., “A Robotics-based Testbed for Verifying a Method of Identifying Contact-Dynamics Model Parameters”, *SPIE Defense and Security Symp*, Orlando, Fl, April 18-21, 2006, Paper #6221-2, p.622102.

[10] Marhefka, D.W. and D.E. Orin, 1999, “A compliant contact model with nonlinear damping for simulation of robotic systems”, IEEE Trans. on Systems, Man, and Cybernetics, Vol.29, No.6, pp.566-572.

[11] Nahon, M., 1994, "Determination of the interference distance between two bodies using optimization techniques", ASME Conf. Advances in Design Auto., Minnesota, Vol.1, pp.1-6.

[12] Liu, C.Y. and Mayne, R.W., 1990, Distance calculations in motion planning problems with interface situations, Proc. ASME Design Eng. Tech. and Auto. Confs., Chicago, Illinois, pp.145-152.

[13] O’Rourke, J., 1993, Computational Geometry in C, Cambridge University press, Cambridge.

[14] Preparata, F. P., and Shamos, M.I., 1985, Computational Geometry: an introduction, Springer-verlag, New York.

[15] Seraji, H., and Colbaugh, R., 1997, “Force tracking in impedance control,“ International Journal of Robotics Research, Vol. 16, No. 1, pp. 97-117.

[16] Song, P., Kraus, P., Kumar, V., and Dupont, P., 2001, “Analysis of rigid-body dynamic models for simulation of systems with frictional contacts”, ASME Trans., J. of Appl. Mech., Vol.68, pp.118-128.

[17] Stoianovici, D. and Hurmuzlu, Y., 1996, A critical study of the applicability of rigid-body collision theory, ASME, J. of Applied Mech., Vol.63, pp.307-316.

[18] Stronge, W.J., 2000, Impact Mechanics, Cambridge University Press, London.

[19] Weber, M., Patel, K., Ma, O., and Sharf, I., 2006, “Identification of contact dynamics model parameters from constrained robotic operations”, *ASME J. of Dyn. Syst., Meas., and Ctrl*, Vol.128(2), 2006, pp.307-318.

[20] Van Vliet, J., Sharf, I. and Ma, O., 2000, “Experimental validation of contact dynamics simulation of constrained robotic tasks”. International Journal of Robotics Research, Vol.19, No.12, pp.1203-1217.

[21] Vukobratovic, M.K. and Potkonjak, V., 1999, “Dynamics of contact tasks in robotics. Part I: general model of robot interacting with environment”, Mechanism and Machine Theory, Vol.34, pp.923-942.